The REX survey: a search for Radio Emitting X-ray sources.

Alessandro Caccianiga¹, Tommaso Maccacaro, Anna Wolter, Roberto Della Ceca, Osservatorio Astronomico di Brera, Via Brera 28, I-20121 Milano, Italy

and

 ${\rm Isabella~M.~Gioia}^2$ ${\rm Institute~for~Astronomy,~2680~Woodlawn~Drive,~Honolulu,~HI,~96822~USA}$

ABSTRACT

We present the scientific goals, the strategy and the first results of the REX project, an effort aimed at creating a sizable and statistically complete sample of Radio Emitting X-ray sources (REX) using the available data from a VLA survey (NVSS) and the ROSAT PSPC archive. Through a positional cross-correlation of the two data sets we have derived a sample of about 1600 REX. Among the 393 REX identified so far (either from literature or from our own spectroscopic observations) a high fraction is represented by AGNs (about 60 - 80%), typically radio loud QSOs and BL Lacs. The remaining sources are galaxies, typically radio galaxies isolated or in cluster. Thanks to the low flux limits in the radio (5 mJy at 1.4 GHz) and in the X-ray band ($\sim 5 \times 10^{-14} \text{ erg s}^{-1} \text{ cm}^{-2}$, 0.5–2.0 keV) and the large area of sky covered by the survey (2183 deg²), we intend to derive a new complete and unbiased sample of BL Lacs which will contain both "RBL" and "XBL" type objects. In this way, the apparent dichotomy resulting from the current samples of BL Lacs will be directly analyzed in a unique sample. Moreover, the high number of BL Lacs expected in the REX sample (~ 200) will allow an accurate estimate of their statistical properties, like the X-ray, radio and optical luminosity functions and the cosmological evolution. For these reasons, the REX sample will be a powerful tool to test accurately the current theoretical models proposed for BL Lacs. To date, we have discovered 15 new BL Lacs and 11 BL Lac candidates with optical properties intermediate between those of a typical elliptical galaxy and those of a typical BL Lac object. These objects could harbour weak sources of non-thermal continuum in their nuclei and, if confirmed, they could represent the faint tail of the BL Lac population. The existence of such "weak"

¹Present Address: Observatorio Astronomico de Lisboa, Tapada da Ajuda, P-1300 Lisboa, Portugal

²also Istituto di Radio Astronomia del CNR, via Gobetti 101, 40129 Bologna, Italy

BL Lacs is matter of discussion in recent literature and could lead to a re-assessment of the defining criteria of a BL Lac and, consequently, to a revision of their cosmological and statistical properties.

Finally the sample of ~ 800 Emission Line AGNs, resulting from the REX survey, will be useful in addressing many of the open questions regarding the AGN phenomenology like the relationship between radio loud and radio quiet AGNs.

Subject headings: surveys - galaxies: active - quasar: general - BL Lacertae objects: general

1. Introduction

The optical identification of radio or X-ray catalogs is instrumental in deriving large samples of AGNs (e.g., Stocke et al. 1991, Boyle et al. 1994, Page et al. 1996 for the X-ray band and Gregg et al. 1996 for the radio band). In these years, new radio and X-ray surveys characterized by low flux limits and a wide coverage of the sky are in progress. In the radio band there are two similar projects aimed at creating new catalogs of radio sources at mJy fluxes with accurate radio positions (few arcseconds of uncertainty or better) based on VLA observations, i.e. the NRAO VLA Sky Survey (NVSS, Condon et al. 1998) and the Faint Image of Radio Sky at Twenty centimeters survey (FIRST survey, Becker et al. 1995). The NVSS survey covers all the sky north of $\delta = -40^{\circ}$ using the VLA D and DnC configurations, with a typical rms of 0.45 mJy; the FIRST survey covers about 10,000 deg² around the North Galactic Pole plus a southern strip (from RA = $21^h \ 20^m \ \text{to} \ 3^h \ 20^m \ \text{and from Dec} = -2.5^{\circ} \ \text{to} \ 1.6^{\circ}$) with a higher spatial resolution (B configuration) and a lower flux limit (rms ~ 0.15 mJy) with respect to the NVSS. Eventually, both catalogs will contain more than 10⁶ radio sources each. In the X-ray band, the ROSAT satellite has produced a great bulk of data, both from the All Sky Survey (RASS) and from about 4000 PSPC pointed images gathered into public archives. The first catalog of bright (f_{[0.1-2.4]keV}>10^{-12}~\rm erg~s^{-1}~cm^{-2}) X-ray sources produced by the RASS contains about 19,000 sources (Voges et al. 1996), while the catalogs derived on the basis of public pointed PSPC images (WGA catalog, White, Giommi and Angelini, 1994 and ROSATSRC catalog, ROSAT NEWS n.32, 1994) contain about 70,000 sources each. All these surveys offer a great opportunity to derive new sizable samples of AGNs. In particular, the RASS and the VLA surveys will be useful to perform detailed statistical analyses. On the other hand, the large numbers of sources contained in these catalogs draw the attention to the problem of the optical identification. Even with the high positional accuracy of the VLA, which guarantees the (almost) univocal identification of the correct optical counterpart (at least for $m_V < 20$), the number of optical candidates to observe spectroscopically is undoubtedly high. This number increases dramatically in the case of the X-ray catalogs derived from the ROSAT PSPC data, which are characterized by larger positional errors (typically from 14" to 50", see § 4.3). As a consequence, the completion of the optical identification process of these surveys will

require decades. This fact points out the importance of finding efficient pre-selection techniques to extract from the whole sample only the candidates of interest for spectroscopic follow up. Many authors have initiated specific efforts aimed at creating samples of AGNs from VLA data (Gregg et al. 1996) or BL Lacs from ROSAT data (Perlman et al. 1998; Laurent-Muehleisen et al. 1998; Nass et al. 1996; Kock et al. 1996) through the application of particular pre-selection criteria based on radio-to-optical or X-ray-to-optical flux ratios, or using information on optical polarization.

The primary goal of the REX project is the selection of a *statistically complete* sample of AGNs, in particular radio loud (RL) QSOs and BL Lacs, by using *simultaneously* the information derived from the NVSS survey and from pointed ROSAT PSPC images. Through a positional cross-correlation of sources detected in the NVSS and ROSAT fields, we derive a sample of *Radio Emitting X-ray sources (REXs)* which is expected to contain a high fraction of AGNs (radio loud QSOs, BL Lacs, Seyfert galaxies) and radio galaxies. This method has two fundamental advantages:

- 1) We are able to minimize "a priori" the presence in the sample of objects like stars or "normal" galaxies, which are not strong radio emitting X-ray sources, increasing in this way the efficiency of finding the sources of interest (BL Lacs, QSOs) to be observed spectroscopically;
- 2) We can use the accurate VLA positions to pinpoint the optical counterparts of the X-ray sources.

In this paper, we discuss the main scientific goals of the project (§ 2) and the catalogs of radio (§ 3) and X-ray sources (§ 4) used for the cross-correlation. In § 5 we discuss the source selection criteria and the estimated content of the REX survey. The strategy of optical identification of the sample is described in § 6 while the discussion of the content of the REX sample is reported in § 7. In § 8 we report preliminary results derived from the study of the sample of BL Lacs discovered so far. Our conclusions are summarized in § 9.

Throughout the paper, the values of $H_0 = 50 \text{ Km s}^{-1} \text{ Mpc}^{-1}$ and $q_0 = 0$ are used.

2. Scientific goals

The main goal of the project is the study of RL AGNs and BL Lacs objects. These kinds of AGN are either intrinsically few (RL AGNs are about 10% of the whole class of AGN ³ while BL Lacs represent only few percent) and/or hard to find. BL Lacs, in particular, lack a UV excess or any other peculiar optical spectral signature and, for these reasons, they are found with difficulty

³This is true in the optically selected samples, while in the X-ray selected samples, e.g. in the EMSS sample, the fraction of RL AGNs ranges from 3% to 30%, depending on the optical luminosity (e.g. Della Ceca et al. 1994). We consider radio loud an AGN with $\alpha_{ro} > 0.35$ (see Della Ceca et al. 1994), where $\alpha_{ro} = log(S_{5GHz}/S_{2500A})/5.38$.

in the optical band. Nevertheless, they are both radio loud and X-ray-loud (e.g. Stocke et al. 1990) and, as a consequence, they are typically selected in the X-ray or in the radio band. The small numbers of BL Lacs or RL AGNs available in current complete samples (e.g. the EMSS catalog contains only 36 BL Lacs and 43 RL AGNs, Morris et al. 1991, Della Ceca et al. 1994 and the 1 Jy catalog contains only 34 BL Lacs, Stickel et al. 1991) limits any detailed statistical analysis of these objects. On the other hand, accurate statistical studies are instrumental in order to address the many open questions, like the origin of the differences between radio loud and radio quiet AGNs (e.g. Wilson & Colbert 1995), the supposed dichotomy of the BL Lac population (e.g. Giommi & Padovani 1994, Padovani & Giommi 1995), the cosmological properties (evolution, luminosity functions) of BL Lacs and the problem of their parent population (e.g. Urry & Padovani 1995 and references therein). Many of these questions, in particular those related to BL Lacs, require a significant enlargement of the available complete samples. Moreover, many crucial predictions of the current theoretical models, like the relative number of radio selected (RBL) and X-ray selected (XBL) types (Giommi & Padovani 1994, Fossati et al. 1997), could be verified only by reaching low X-ray flux limits (typically a few 10^{-14} erg s⁻¹ cm⁻²). The REX sample will possess these requirements, as it will contain $\gtrsim 200$ BL Lacs down to a flux limit of $\sim 5 \times 10^{-14}$ ${\rm erg~s^{-1}~cm^{-2}}$ in the 0.5-2.0 keV energy band.

3. The radio catalog

The NRAO VLA Sky Survey began in 1993 and covers now the whole sky north of $\delta = -40^{\circ}$ ($\sim 10.3 \text{ sr}$, 82% of the total sky). It is performed at 1.4 GHz using the compact D and DnC configurations of the Very Large Array in Socorro (New Mexico, USA). The primary product of this survey is a set of 2326 $4^{\circ} \times 4^{\circ}$ maps containing information about total-intensity and linear polarization (Stokes parameters I, Q and U). The size of the restoring beam ($\theta = 45''$ FWHM) allows us to achieve a high surface-brightness sensitivity needed for completeness and photometric accuracy. The rms of the Stokes I maps is $\sigma \sim 0.45 \text{ mJy beam}^{-1}$. The final maps are released electronically by anonymous FTP. Moreover, NRAO extracts a catalog of discrete sources and components (if the radio source is resolved by the VLA beam) detected in the images, by fitting elliptical Gaussian to all significant peaks. The entries consist of a single Gaussian model fits. The sources (or components) are identified in the Stokes I images and then the associated polarization information is derived from the Stokes Q and U images. A brief description of this catalog is given at the WWW home page of NVSS (http://www.cv.nrao.edu/~jcondon/nvss.html). A related program (NVSSlist) is also provided in order to read the catalog (which is released in FITS format) and to browse selected portions of the sky. NVSSlist corrects also the raw catalog for known biases and computes errors associated to the source model parameters (position, flux density, etc.). Both catalog and program are continually updated. For what concerns the REX project, we set the radio limiting flux to 5 mJy (about 10 times the rms of the I maps) in order to achieve accurate positions (95% error circles smaller than 5") and to guarantee the completeness of the sample (see Condon et al 1998 for details). We have used version 2.8 of the NVSSlist program and the version 28 (01/19/98) of the catalog. In that version the NVSS was plagued by a number of holes, i.e. regions of missing data. We have estimated that in the region of sky covered by the X-ray catalog (see section 4) the area lost due to the holes is about 5-7%.

4. The X-ray catalog

The X-ray catalog used for the REX project has been derived from the ROSAT archive of pointed PSPC images. To date, the ROSAT PSPC archive represents the best set of data to derive a large catalog of X-ray sources covering a wide angle of the sky and reaching faint limiting fluxes (below 10⁻¹⁴ erg s⁻¹ cm⁻² in the 0.2 - 2.4 kev band with the deepest images)⁴. We briefly describe the PSPC archive and the existing X-ray catalogs derived from these data. Since these catalogs are not suitable for our purposes, we have undertaken to reanalyze all the PSPC images suitable for this project with the aim of constructing a new statistically representative catalog of sources. We present the selection of the fields used in this project, the process of source detection and the source positional uncertainties in the resulting X-ray catalog.

To date, all the pointed ROSAT PSPC observations (~4000 in total) are of public domain and they are stored in a public archive. The large field of view of the PSPC (about 2.8 deg²) makes this archive of images particularly useful to build up an X-ray catalog of serendipitous sources. Two different catalogs of X-ray sources detected in a number of ROSAT PSPC images have been made public in the past years: the WGA catalog (White, Giommi and Angelini, 1994, IAU Circular 6100) and the ROSATSRC catalog (ROSAT NEWS n.32, 1994). The detection technique used for the WGA catalog is based on a sliding box algorithm which is optimized for point-like sources. The inner (0'-19') off-axis angle and outer (18'-55') off-axis angle regions of the images were processed separately to maximize the sensitivity to source detection. The latest version (rev. 1) of the catalog contains about 68,000 sources detected in 3007 fields. The ROSATSRC catalog is the First Source catalog of pointed observations created at Max Planck Institut für Extraterrestrische Physik. A maximum likelihood detection algorithm was used for the central 20' of the PSPC field and a sliding box algorithm of fixed width was used at larger off-axis angles. About 74,000 sources are contained in the latest version of the catalog (rev. 1) which is derived from the analysis of 3348 fields. Although the bulk of the images used are the same for both catalogs, there are significant differences, probably related to the different methods and thresholds used for the source detection (see White, Giommi and Angelini 1995, in the WGACAT WWW home page (http://lheawww.gsfc.nasa.gov/users/white/wgacat/wgacat.html) for a brief description of these differences). Both WGACAT and ROSATSRC catalogs were created principally to quickly derive a list of X-ray sources useful, for instance, to find peculiar and interesting objects (e.g. sources

 $^{^4}$ The RASS, although it covers the whole sky, reaches limiting fluxes of about 10^{-12} erg s⁻¹ cm⁻² (the Bright RASS catalog) or fluxes of about $1-5\times10^{-13}$ erg s⁻¹ cm⁻² (the total catalog of 60,000 sources presented in Voges, 1993) and, for this reason, it is not optimized to study the faint tail of the LogN-LogS of BL Lacs and RL AGNs.

with anomalous temporal variability or spectral properties) to be re-observed, if necessary, with ROSAT or other telescopes (for example ASCA). For this reason, they were created without a particular attention to the problem of completeness and representativeness. Both catalogs contain. for example, several repetitions, i.e. the same source may appear more than once in the two catalogs: for instance, about 4000 sources in the last version of WGACAT are redundant. This problem is related to the fact that many PSPC pointings overlap one to another and a source may thus be detected separately in two different images. Moreover, the algorithms chosen for the source detection work on a fixed scale while the PSF of the PSPC changes considerably and continuously with the off-axis angle; this problem still holds even when using a different scale in the inner and in the outer region of the PSPC. All these problems make the definition of a complete sample and the derivation of the sky-coverage very difficult for both catalogs. Finally, WGA and ROSATSRC catalogs are not purely made of serendipitous sources because they contain all the targets of the PSPC pointings, affecting the representativeness of the two catalogs. For these reasons, WGACAT and ROSATSRC, although useful for some specific purposes, are not suitable for statistical studies and, in particular, for our project, which requires completeness and representativeness besides a precise estimate of the sky-coverage.

Thus, we have reanalyzed a well defined subset (see § 4.1) of the public PSPC observations with the purpose of constructing a complete and well defined sample of X-ray sources. In particular, we pay attention:

- 1) to resolve the problem of overlapping PSPC images;
- 2) to eliminate all the targets and the target-related sources from the catalog;
- 3) to use a detection algorithm sensitive to the changing of the PSF over the PSPC field;
- 4) to compute the appropriate sky coverage.

4.1. Selection of ROSAT PSPC fields

From the ~ 4000 PSPC images in the public archive, we have selected all the fields that fulfill the following criteria:

- 1) $\delta \geq -40^{\circ}$ (to match the NVSS sky coverage);
- 2) $|b^{II}| \ge 10^{\circ}$ (to avoid the galactic plane);
- 3) exposure time $\geq 1000s$;
- 4) processed with the revision 7 of the SASS as of December 1997 (to use data with an improved aspect solution).

Moreover, we have excluded intrinsically "confused" regions like those with a high stellardensity (e.g. images pointed at Pleiades, Hyades) or near extended dark or molecular clouds, which could create problems in the process of source optical identification or in the computation of the limiting sensitivity of the field.

The distribution in the sky of all the PSPC pointings clearly shows that there are several overlapping images (deep surveys, targets which cover a wide area of sky, fields pointed to close targets). Combining these images in single frames would create several problems during the process of source detection. Typically, the presence of strong gradients in the sensitivity profile of the final image, induced by the edges of the individual fields, creates difficulties to the background determination and to the detection algorithm and may yield spurious sources. We avoided this problem simply by excluding from the analysis the outer region of one of the overlapping fields in order to obtain a mosaic of separated fields. Figure 1 illustrates this "cleaning" procedure.

Finally, in the case of exact overlap in sky coordinates of two or more distinct pointings, we summed them and we considered these fields as a single image with an exposure time which is the sum of the individual exposures. In this case, the name of the resulting field is formed by the lowest ROSAT Observation Request (ROR) sequence number with the suffix "sum".

In order to achieve a catalog of purely serendipitous sources, we have eliminated from the survey the area containing the target of the observation (since it is, by definition, not chosen randomly) and all the target-related sources. In the majority of the PSPC pointings, the target falls in the center of the field and its extent is typically included in a circle of 4' radius. In the case of images pointed toward rich/nearby clusters of galaxies, the radius of the circle around the target can be considerably larger (from 10' to 20'). The few fields which contain very extended targets (dimension $\geq 25'$) have been fully excluded from the survey. In the few cases in which the target object was deliberately off-set from the center (e.g. for variability studies) we excluded a circle of radius r_t centered on the target position. Furthermore, in the case of PSPC images centered on an optically very bright object (e.g. α Ari, β CMa), we have excluded the area "blinded" by the optical image. In these cases, in fact, it would be extremely difficult, if not impossible, to optically identify a serendipitous source close to the target.

In total, we have selected 1202 distinct PSPC fields. For reference, we have made electronically available⁵ a table containing the complete list of PSPC images used for this survey covering a total area of 2183 deg². In particular, we have reported, for each PSPC field, the Rosat Observation Request sequence number (ROR), the sky coordinates (J2000), the exposure time (which is the total exposure time in the cases of summed fields), the inner (r_i) and the outer (r_o) radius of the PSPC region used, the position of the target in detector coordinates and the radius of the excluded area $(X_t, Y_t \text{ and } r_t)$ if the target is off-set and the Galactic hydrogen column density (in units of 10^{20} cm^{-2}) derived from Dickey & Lockman (1990). When there were no targets (e.g. surveys or mispointed fields) both r_i and r_t are zero. The maximum value of the outer radius has been set

⁵ The table pspc_table.txt can be retrieved by "anonymous" ftp at *ftp.brera.mi.astro.it*. The table (in ASCII format) is in the directory "/pub/REX/tables/". A description of the table is found in the file pspc_table.doc in the same directory.

to 47' (although the "standard" radius of a PSPC field is 55') in order to exclude the part of the PSPC where the PSF degradation is severe and the positional uncertainties are too large (> 50'').

We report in Figure 2 the distribution in the sky of the total set of selected PSPC fields while in Figure 3 we show the histogram of their exposure times.

4.2. The detection algorithm

The detection algorithm used for this project was developed at the Palermo Astronomical Observatory and it is described in detail in Damiani et al. 1997a. The method is based on wavelet transforms, that are well suited to the case where the Point-Spread Function (PSF) is varying across the image (see also Rosati et al. 1995). This detection technique outperforms that used to produce the WGA and the ROSATSRC catalogs in terms of reliability and efficiency.

For the REX project, we have applied the detection algorithm to the selected set of PSPC fields, using the "hard" images (0.5 - 2.0 keV) to reduce the intensity of the background and to minimize the effects due to Galactic absorption. Moreover, the choice of the hard band minimizes the uncertainties related to the conversion from count-rate to flux due to the unknown spectral shape of the sources, as discussed in Vikhlinin et al. (1995). The images used have 15" pixel size. The final catalog contains 16,275 X-ray sources detected with a confidence level $\geq 6\sigma$ (see Damiani et al. 1997a for a discussion on the determination of the probability associated to a given source detection threshold) and a count-rate $\geq 3 \times 10^{-3}$ cts/s. The high threshold on significance guarantees a very low number of spurious X-ray sources (see Figure 3 of Damiani et al. 1997b); the limit on the count-rate was chosen to avoid very faint sources that could be very difficult to identify spectroscopically. Assuming a power-law spectrum with an energy index $\alpha_X = 1.0 \ (f_{\nu} \propto \nu^{-\alpha})$ this count-rate limit corresponds to a limiting flux in the 0.5-2.0 keV band of $\sim 3.5 \times 10^{-14}$ erg s⁻¹ cm⁻², for $N_H = 7 \times 10^{19}$ cm⁻² (the lowest value for the PSPC fields used in the REX survey) and of $\sim 6 \times 10^{-14}$ erg s⁻¹ cm⁻² for $N_H = 2 \times 10^{21}$ cm⁻² (the highest value).

4.3. The positional accuracy of the X-ray catalog

Before cross-correlating the X-ray catalog with that derived from the NVSS survey, it is crucial to accurately assess the positional uncertainties. The error circle of the sources detected in the ROSAT PSPC images is typically of the order of tens of arcseconds while the error circles associated with the NVSS positions are an order of magnitude smaller (few arcseconds). Therefore, the impact parameter, which is the square combination of the two error circles, depends mainly on the X-ray positional accuracy.

To determine the uncertainties associated with the X-ray positions, we have cross-correlated the X-ray sources against two catalogs: the Hipparcos Input catalog of stars (HIC, Perryman et

al. 1997) and the V&V96 catalog of AGNs (Véron-Cetty & Véron 1996).

The HIC catalog contains 118000 stars with a positional accuracy of $\sim 0.3''$. In the case of the V&V96 catalog we have used only the 8272 sources with a good estimate of the position (accuracy better than 1").

By using an impact parameter of 4' we found 960 X/V&V96 correlations and 525 X/HIC correlations for a total of 1485 sources. The distribution of the offsets in right ascension ($\Delta\alpha$) and in declination ($\Delta\delta$) between the X-ray and the V&V96 or HIC positions is shown in Figure 4. We have divided the sources in three groups, corresponding to different ranges of the offaxis angle (θ): (a) from 0' to 19'; (b) from 19' to 35'; (c) from 35' to 47'.

Using two different methods, we have estimated from these data the positional errors of the X-ray sources as a function of the offaxis angle.

In the first method we compute, from the three panels presented in Figure 4 the radius of the circle that includes 90% of the *real* positional correlations (the total correlations minus the expected chance coincidences), i.e. the radius (r_{90}) of the circle which contains 90% of the points is defined by:

$$\frac{N(\leq r_{90}) - N_{sp}(\leq r_{90})}{N_{tot} - N_{spTOT}} = 0.90$$
 (1)

where:

 $N(\leq r_{90})$ is the number of correlations with offset $\leq r_{90}$;

 $N_{sp}(\leq r_{90})$ is the number of expected spurious correlations with offset $\leq r_{90}$;

 N_{tot} is the total number of correlations within the 4' radius;

 N_{spTOT} is the total number of expected spurious correlations within the 4' radius;

We have estimated N_{sp} and N_{spTOT} by assuming that all the sources with an offset $> r_{sp}$ were of spurious origin. The value of r_{sp} ranges from 50", for $\theta \le 19$ ', to 100", for $35' \le \theta \le 47$ '. This analysis indicates that the error circles at the 90% confidence level are: 14" for $\theta < 19$ ', 40" for $19' \le \theta < 35'$ and 50'' for $35' \le \theta \le 47'$.

Alternatively, we have studied the differential distribution of the number of correlations found, defined as:

$$d(r) = \frac{N(r, r + \delta r)}{\pi \times [(r + \delta r)^2 - r^2]}$$
(2)

where:

 $N(r, r + \delta r)$ is the number of correlations with offset between r and $r + \delta r$;

 δr is the width of the bin used (=2").

Then, we have performed a fit to this distribution using a Gaussian profile, assumed to represent the real coincidences, plus a constant, representing the spurious matches. The radius of the 90% error circle is then obtained by the σ of the Gaussian fit. The problem related to this method is that the observed profiles typically are not Gaussian, showing a systematic excess (wings) at large values of r. Moreover, the first bins contain few objects so that the uncertainties are large. By excluding the first 3 bins from the analysis we have found values of the r_{90} in good agreement with those estimated with the first method.

In conclusion, for the positional cross-correlation we use an X-ray error circle of radius 14", 40'' and 50'' for $\theta < 19'$, $19' \le \theta < 35'$ and $35' \le \theta \le 47'$ respectively.

5. The REX selection

5.1. Criteria for the cross-correlation

Given the estimate of the X-ray and radio positional error circles, the impact parameter (b) to be used during the cross-correlation to achieve the 90% completeness level can be determined simply by summing quadratically the two positional uncertainties $(\sigma_R \text{ and } \sigma_X)$ corresponding to the 90% confidence level for the radio and the X-ray positions, i.e.:

$$b = \sqrt{(\sigma_R^2 + \sigma_X^2)} \tag{3}$$

In practice, $\sigma_R^2 \ll \sigma_X^2$ (see Condon et al. 1998 and § 4.3) and thus $b \sim \sigma_X$. Since we use the 90% confidence level error circles, we expect to lose about 10% of the REXs using the impact parameter given by equation (3). This represents a compromise between reliability and completeness since a larger value of b would increase the number of spurious radio/X-ray correlations while a smaller value of b would increase the number of missed REXs. Clearly, the loss of 10% of the REXs has to be considered when deriving the statistical properties like the LogN-LogS or the luminosity function.

A positional cross-correlation between the radio and the X-ray catalogs using the impact parameter b given in equation (3) is the correct way to find REXs which are unresolved in the radio band. However, a large number of radio sources (e.g. radio galaxies and radio loud QSO) show characteristic extended structures (radio lobes, cores, jets) often well resolved in VLA images, even with the compact D and DnC configuration used for the NVSS. In these cases, the X-ray emission is centered in correspondence of the radio core and may be distant from the emission of the other structures (radio lobes). In a number of cases only the emission produced by the lobes is visible on the radio map and the object appears as a double radio source. As a consequence, several REXs (typically quasars and radio galaxies) could be lost in a "blind" positional cross-correlation. The absence of a radio core in radio loud QSO is a well-know possible cause of incompleteness

which may affect in particular the highly resolved VLA surveys. For example this effect can be one of the principal sources of incompleteness for the FIRST bright QSO survey (Gregg et al. 1996). The existence of double radio sources may introduce also an erroneous identification of the optical counterpart of the REXs in the case in which only one radio component falls inside the X-ray error circle: in this case the REX is not lost but the optical counterpart, if it is supposed to be coincident with the radio position, could be misidentified or could be spurious. In Figure 5, four cases of two NVSS components (small circles) close to the X-ray position (large circle) are presented. We note that the size of the X-ray error circles depends on the offaxis angle, as described in section 4.3, while, for clarity, the radio error circles are all plotted with a fixed size of 6". Figure 5a is an example of a possible double radio galaxy whose lobes lie just outside a X-ray error circle, which contains the optical galaxy. If we cross-correlate using the impact parameter "b" defined above (eq.[3]) this source would be lost. Figures 5b and c are similar cases of possible double radio galaxies in which one of the two components lies inside the X-ray error circle. In both cases the source would be selected as a REX but a search for the optical counterpart at the radio position of the component consistent with impact parameter "b" would fail to produce the correct identification. In the case of Figure 5b the REX is correctly retained in the sample, while in Figure 5c the match would be spurious since the optical counterpart of the radio source is not consistent with the X-ray position. Finally, Figure 5d shows a false case of double radio source: one of the two components is a radio source consistent with X-ray position, while the second one is an unrelated radio source. Given this complex situation, instead of cross-correlating with the parameter "b" we use the following procedure. We cross-correlate the two catalogs using a large impact parameter (2.5'); this yields a large list of positional coincidences, most of which of spurious origin. At this stage, double radio sources are not missed (if their sizes are less than $\sim 5'$), but we have to deal with the problem of separating the real coincidences from the spurious ones. The possible cases can be divided in three categories schematically represented in Figure 6:

- Case 1: only one radio source falls closer than 2.5' to an X-ray source;
- Case 2: two radio sources fall closer than 2.5' to an X-ray source;
- Case 3: three or more radio sources fall closer than 2.5' to an X-ray source.

The first case is the simplest to deal with: if the radio and X-ray positions are consistent within the impact parameter defined by equation (3) we consider this object a REX; otherwise we eliminate the source.

We call the other two cases T-REX, for *Temporary REX*. The number of T-REX is very large, because of the large impact parameter used for the cross-correlation, and, for this reason, we filter automatically some obvious cases of chance coincidences. In particular, we can exclude "a priori" situations in which the line joining the two radio positions does not intersect the X-ray error circle, i.e., the optical counterpart of the presumed double source falls outside the X-ray error

circle ⁶ (see Figure 6, case 2d) or, if it intersects the X-ray error circle, both the radio components are on the same side. By excluding all these situations (in case 2) we reduce significantly the number of T-REXs which have to be considered. For the remaining cases, we inspect the $5' \times 5'$ optical finding chart from the Digitized Sky Survey (DSS)⁷ and the $5' \times 5'$ radio map produced from the NVSS images and we try to detect all the possible cases of radio extended REXs and to recognize sources that are clearly chance coincidences (considering the position of the plausible optical counterpart and the morphology of the radio emission). We have analyzed the sample of ~ 1000 T-REXs resulting from the cross-correlation and we have found that, on the basis of the radio and optical maps, we are able to distinguish a real REX from a chance coincidence in $\sim 80\%$ of the cases. The other 20% T-REXs will be correctly classified only after gathering further information including the spectroscopic data for the possible optical counterparts. Of the T-REXs that we have already classified 90 are real double or triple radio sources (see Figure 5a), 443 are represented by "normal" REXs, i.e. the radio source consistent with the X-ray position is not related to the other radio component(s) found within 2.5' (see Figure 5d) and 318 are chance coincidences i.e. the radio and the X-ray sources are not related.

The source catalog containing the relevant information on the REXs (position, X-ray and radio flux and relative errors, etc.) will be made available electronically ⁸ as soon as the NVSS data become stable and the REX quality check is completed. At the time of this writing the NVSS catalog is still an evolving entity because of the existence of a few snapshot fields lacking total intensity images (corresponding to about 5-7% of the area covered by the X-ray data). These gaps are being filled by the NVSS group either by re-processing of existing data or by new observations. We anticipate that we will release a REX catalog obtained using the latest NVSS version and thus the total number of sources will differ marginally from that presented in this paper. Furthermore, for each REX we intend to make available an optical finding chart derived from the DSS.

5.2. Estimate of the number of radio/X-ray chance coincidences

We can evaluate the number of chance coincidences produced by the X-ray/radio cross-correlation in two different ways. One possibility is to calculate the number of spurious REXs

⁶ In principle this criterion could exclude from the sample a fraction of the sources where the optical counterpart (or the radio core) is not aligned with the two radio lobes (e.g. Wide Angle Tail - WAT - sources). However, the number of X-ray emitting WAT sources is not large: by performing the cross-correlation using a larger tolerance (e.g. 1.5×b) we have not found any evidence of possible Wide Angle Tail source. Therefore we are confident that this bias is not important in the REX sample. Moreover we remind that complex radio morphologies, i.e. sources with three or more NVSS components, are all retained as T-REX and visually inspected afterward.

 $^{^7}$ The Digitized Sky Survey is produced at the Space Telescope Science Institute (STScI) under U.S. Government grant NAG W-2166

 $^{^8}$ A status report on the REX project (README.REX) can be retrieved by "anonymous" ftp at $\it ftp.brera.mi.astro.it$ in the directory "/pub/REX".

analytically, i.e. computing the number of radio sources expected by chance within a circle of radius "b" centered on an X-ray position. If N_1 , N_2 and N_3 are the number of X-ray sources with $\theta < 19'$, $19' \le \theta < 35'$ and $35' \le \theta \le 47'$, respectively, and b_1 , b_2 and b_3 are the corresponding impact parameters used for the cross-correlation, the total number of expected chance coincidences is:

$$N_{chance} = (N_1 \times \pi b_1^2 + N_2 \times \pi b_2^2 + N_3 \times \pi b_3^2) \times \rho \tag{4}$$

where ρ is the number of radio sources per unit area with a radio flux greater than 5 mJy. We have N_1 =4943, N_2 =7674, N_3 =3658 and $\rho \sim 31$ deg⁻² and, consequently, $N_{chance} = 170$, that is about 10% of the total number of the REXs.

Alternatively, the number of chance coincidences can be derived by cross-correlating the two catalogs after applying a relative shift in position to one catalog: if this off-set is significantly greater than the impact parameter b, we expect that all the results of the cross-correlation are pure chance coincidences. By using this second approach we have derived that the expected percentage of chance coincidences in the REX sample is $11.5\pm2\%$, in agreement with the result of the other (independent) method.

For what concerns the double or triple REXs, the computation of the spurious matches is not so straightforward as for the "single component" REX. On the other hand, these complex sources represent a small fraction (about $\sim 6\%$) of the total number of REX and thus the overall percentage of chance coincidences is practically determined by the "single component" REX.

Finally, we note that the estimated percentage of chance coincidences is a function of the offaxis angle, since the size of the impact parameter used for the cross-correlation depends on the position of the source in the PSPC field. If we consider the three ranges of offaxis angle independently, we find that the percentage of chance coincidences is 2.6% in the inner part of the PSPC field ($\theta \le 19'$), 12% between 19' and 35' and 16% for $\theta \ge 35'$. Thus, upon completion of the identification program, a comparison of the identification content as a function of the off-axis angle will provide information useful for the recognition of the spurious matches.

Moreover, if, during the identification process, we find within the X-ray error circle a source which is a good candidate as optical counterpart of the X-ray source but which is not positionally consistent with the radio source, we flag this REX as a possible spurious match.

5.3. Expected composition of the REX sample

The expected composition of the REX sample depends on the radio, X-ray and optical limits. We estimate that the main constituents of the sample will be RL AGNs and BL Lac objects. Nevertheless, a number of radio quiet (RQ) AGNs is also expected if their magnitudes are sufficiently bright. For instance, a RQ AGN with $\alpha_{ro} = 0.3$ will be included in the REX survey (i.e. it will have a radio flux ≥ 5 mJy) only if its magnitude is brighter than ~ 18 . Also clusters of galaxies will be present in the REX sample, if they contain at least one bright (≥ 5 mJy) radio

galaxy. In this case the term "REX" is somewhat improper because the radio and the X-ray emissions come from physically disjointed (although related) sources (the hot diffuse plasma) in the X-ray band, and the radio galaxy, in the radio band. The number of cluster of galaxies expected in the REX sample is difficult to compute. First of all, there is a strong bias against clusters which do not contain bright radio galaxies. Moreover, even in the case of a cluster containing a powerful radio galaxy, the position of such radio source has to be consistent, within the impact parameter "b", with the position of the center of the X-ray source, that has no relation with the physical dimension of the cluster. Since neither the fraction of clusters containing a bright radio galaxy nor the positional distribution of such radio galaxies within the cluster itself are known accurately, a quantification of these biases is hard to compute. We stress that these considerations imply that the sample of clusters of galaxies selected in this project can not be used for statistical purposes. On the other hand, the REX sample could be very useful to find individual high redshift clusters of galaxies. For the same reasons discussed above, it is difficult to predict the expected number of radio galaxies in the REX survey since a significant fraction of them is found in clusters. Thus, in this section, we will assess the predicted properties only of the AGNs and BL Lacs. To this end, we have used the current knowledge of the statistical properties of these classes of objects (i.e. luminosity functions, evolution, X-ray - optical - radio relationships).

RL AGNs.

The X-ray luminosity function (XLF) and the cosmological evolution of this class of objects have been adapted from Della Ceca et al. (1994). The XLF has been first rescaled from the 0.3-3.5 keV energy band to the 0.5-2.0 keV energy band and then integrated over the luminosity range 10^{42} to 10^{47} erg s⁻¹ and from z=0 to z=4. We have assumed the best-fit evolutionary model until z=2 and no evolution at higher redshift. Given the shape of the XLF (flat at low luminosities and steep at high luminosities) the results of the integration are not particularly sensitive to the choice of the luminosity limits. By convolving the results with the X-ray sky-coverage we have derived a synthetic sample of sources characterized by an X-ray flux and a redshift. Then, we have assumed a relationship between radio and X-ray luminosities and between optical and X-ray luminosities, and we have associated to each object the corresponding radio and optical flux. To this purpose, we have used the correlation between the total (extended plus core) radio luminosities at 1.4 GHz and the luminosities at 2 keV and the relationship between the luminosities at 2500 Å and the luminosities at 2 keV, derived by Brinkmann et al. (1997) for the RL QSO detected in the RASS. We have added a "synthetic" noise to the relationships to mimic the spread of the observed distributions. Finally, we have imposed the radio limit (flux_{1.4GHz} \geq 5 mJy), obtaining an expected sample of ~ 1200 RL AGNs. As previously discussed (section \S 5.1), we expect to loose about 10% of real REX because of the impact parameter used in the cross-correlation. As a consequence, the predicted number of RL AGNs in the REX sample is about 1100. In Figure 7 we show the distributions of radio, X-ray and optical monochromatic luminosities and the redshift distribution for this sample.

BL Lac objects

We have considered the two population of BL Lacs (i.e. XBL-type and RBL-type, see section § 8.2) separately. For both the XBLs and the RBLs we have used the X-ray LFs and the evolutionary parameters presented in Wolter et al. (1994). After rescaling the XLFs to the 0.5-2.0 keV energy band, we have integrated them from 10^{42} to 10^{47} erg s⁻¹ and from z=0 to z=4. We have assumed no-evolution after z=2. From Wolter et al. (1994) we have also used the relationships between the radio and X-ray luminosities and between the optical and X-ray luminosities. Then, as for the RL AGNs, we have imposed the radio limit (flux_{1.4GHz} \geq 5 mJy) to derive the expected sample of BL Lacs. We have obtained a simulated sample of about 290 BL Lacs, 120 of which are XBL and 170 are RBL. Taking into account the 10% of BL Lacs that will be lost during the cross-correlation, the effective number of BL Lacs expected in the REX sample is about 260. The properties of the simulated sample of XBL-type and RBL-type objects are presented in Figure 8. We note that these results are sensitive to the evolutionary parameters and to the luminosity ranges used in the integration of the luminosity functions. Of course, the dependence of the results on the parameters used implies that the final composition of the REX sample will provide strong constraints on the evolutionary properties of BL Lacs as well as on XBL/RBL ratio.

RQ AGNs.

As stated previously, we do not expect a high number of RQ AGNs ($\alpha_{ro} < 0.35$) in the REX sample because of the presence of a relatively high radio flux limit. For a comparison, in the EMSS sample (Maccacaro et al. 1994) only 6 of the 382 RQ AGNs (\sim 2%) have a radio flux (at 5 GHz) above 5 mJy and most are not detected even at 1 mJy. To quantify the number of expected RQ AGNs, we have used the XLF and evolution model of the RQ AGN population as given in Della Ceca et al. (1994), adapted to the 0.5-2.0 keV energy band, and we have integrated the derived XLF from $L_X = 10^{41}$ to 10^{46} erg s⁻¹ and from z=0 to z=4. We have assumed the best-fit evolutionary model until z=2 and no evolution afterwards. The radio (or radio upper limit) and optical flux to be associated to each simulated X-ray source has been computed under the hypothesis that the α_{rx} and α_{ro} distributions of the RQ AGNs in the EMSS sample are representative of the class. The expected number of RQ AGNs in the REX survey obtained after imposing the radio constraint is $\lesssim 100$.

In Figure 9 we show the total number of AGNs (both radio loud and radio quiet, solid line) and BL Lacs ("XBL" + "RBL" type, dashed line) expected in the REX sample as a function of the limiting magnitude, m_B . We note that 70 - 80% of the expected BL Lacs and AGNs are brighter than $m_B = 21$, and thus observable with 4 meter-class telescopes.

6. Optical identification of REXs

The positional accuracy of the VLA data guarantees that there is, in general, only one possible optical counterpart for each REX, at least for $m_B \leq 21$. In the case of a T-REX the

situation is slightly different but in general the objects to observe spectroscopically are at most two. This represents a great advantage over similar projects requiring optical identification of X-ray catalogs derived from PSPC observations and makes the complete identification of the REX sample a feasible endeavor. The importance of dealing with a fully identified sample of sources is fundamental as it was clearly demonstrated by previous such surveys (e.g. the *Einstein EMSS*). Even with a VLA position, however, one should pay attention to the possibility of finding spurious optical candidates falling within the error circle, in particular at faint magnitudes. We have assessed the expected probability of finding interlopers in error circles of 5" and of 2" radius (95% confidence for a NVSS source of 5 mJy and \geq 10 mJy, respectively) using the surface density of stars, galaxies and QSOs at the POSS II limit, as given by Condon et al. (1998). The results are extremely encouraging since the number of spurious objects of all kinds expected is of the order of few percent (radius of 5") or < 1% (radius of 2").

For each REX we create a $5' \times 5'$ finding chart from the DSS material and we search for the probable optical counterpart. Using the NED facility we have identified a number of sources from the literature. At the same time we have initiated spectroscopic observations at the 88'' telescope of the University of Hawaii (UH) in Mauna Kea (USA), at the 2.1m telescope of UNAM in S. Pedro Martir (Mexico) and at the 2.2m and the 3.6m telescopes of ESO (Chile).

The spectroscopic observations have been carried out during the period 1995/1998 using a long-slit and low dispersion (from 3.7 Å/pixel to 13.2 Å/pixel) set-up to maximize the wavelength coverage. The details of the set-up used during the observing runs are summarized in table 1. Details about the individual sources observed at the S. Pedro Martir 2.1m telescope in the period April - September 1995 have been presented in Wolter, Ruscica & Caccianiga (1998).

For the reduction of the data we have used the IRAF longslit package. The spectra have been calibrated in wavelength by using an He–Ar (UNAM, ESO) or a Hg–Cd–Zn (UH) reference spectrum. The photometric standard stars observed for the flux calibration are: Feige 34 (UNAM, UH), BD+284211 (UNAM), HD 19445 (UH), SAO 098781 (UH), LTT 377 (ESO) and HD 84937 (UH). No attempt has been made at performing an absolute photometric calibration.

In total, at the time of this writing, we have observed and identified 125 REX. We have classified the objects on the basis of the features observed in their optical spectrum. We classify a source as $Emission\ Line\ object$ if at least one strong (EW ≥ 5 Å in the source rest frame) emission line is present in the spectrum. Then, on the basis of the width of the observed line(s) we call the object $Broad\ Emission\ Line\ AGN$ if the FWHM of at least one emission line is greater than 1000 km/s (in the rest frame of the source) or $Narrow\ Emission\ Line\ Object$ if all the observed lines have FWHM < 1000 km/s. In this last case we have applied, when possible, the diagnostic criteria presented in Veilleux & Osterbrock (1987) to distinguish a starburst galaxy from an AGN.

In the case of the objects without any strong emission line (EW<5 Å) we have used the relative depression of the continuum across λ =4000 Å (the *Ca II contrast*) as an indicator of the presence of a nuclear non-thermal component (a BL Lac nucleus) in the host galaxy. We have

computed its amplitude following Dressler & Shectman (1987), i.e. by estimating the average fluxes (expressed in unit of frequency) between 3750 Å and 3950 Å (f^-) and between 4050 Å and 4250 Å (f^+) in the rest-frame of the source; the contrast is then defined by:

$$K(Ca\ II) = \frac{f^{+} - f^{-}}{f^{+}} \tag{5}$$

If this feature is absent or if it has an intensity less than 25%, the optical emission of the source is dominated by the non-thermal nucleus and we define the object as firm BL Lac according to the usual definition (e.g. Stocke et al. 1991). This limit had been proposed on the basis of the study of the spectroscopic properties of a sample of (mostly) elliptical galaxies presented in Dressler & Shectman (1987). Stocke et al. (1991) pointed out that only 1.2% of the galaxies contained in the Dressler & Shectman sample have K(Ca II) < 25% (and no emission lines with EW > 5 Å) and that, consequently, it is extremely unlikely that normal elliptical galaxies would be classified by mistake as a BL Lac object, by using these definition criteria. Moreover, the adopted classification was supported by the absence, in the EMSS sample, of objects without emission lines (EW<5 Å) and with a Ca II contrast between 30% and 40% (see Figure 4 in Stocke et al. 1991). In the last years, however, after the discovery of a large number of new BL Lacs from the identification of the ROSAT All Sky Survey catalog (Laurent-Muehleisen et al. 1998) or from a sample of optically bright flat spectrum radio sources (Marchã et al. 1996), this "gap" has been partially filled up and the distinction between a "normal" elliptical galaxy and a BL Lac object has become blurred, at least in the optical band. Therefore it is necessary a re-definition of the classification criteria used to distinguish a BL Lac from an elliptical galaxy. To this end, we have studied the objects found in the REX sample without optical emission lines and with a measurable Ca II contrast. In Figure 10 we have reported the observed distribution of the values of Ca II contrast for this sample of sources. The histogram is peaked around K(Ca II)~50\%, that is consistent with the mean value found by Dressler & Shectman (1987) for a population of elliptical galaxies. However, unlike the Dressler & Shectman sample, where only 5\% of galaxies have a K(Ca II)\le 40\%, our sample contains 18 objects out of 46 (39%) with a K(Ca II) < 40%. This excess is statistically significant $(\geq 5\sigma)$ and it is also present in the samples studied by Laurent-Muehleisen et al. (1998) and Marchã et al. (1996). We consider this excess as evidence of the presence, at least in the objects with K(Ca II)<40\%, of an extra source of continuum that lowers significantly the values of the Ca II contrast. Also the objects with K(Ca II)>40% could, in principle, harbour an optically weak BL Lac nucleus, whose intensity is not sufficient to reduce significantly the value of Ca II contrast. We are not able to distinguish these cases using only our optical discovery spectra. The lack of a sharp bimodality in the Ca II contrast distribution makes the problem of the definition of a BL Lac a task somewhat arbitrary (at least using only optical spectroscopy). On the other hand, as discussed in section § 8.1, the existence of objects intermediate between a typical BL Lac and a typical radio galaxy is of fundamental importance in the context of the "beaming model" and should be investigated with attention.

Nevertheless a limit on the value of Ca II contrast to distinguish a BL Lac from a galaxy is

needed, at least, from an operative point of view. While it is now clear that the usual limit of 25% fails to find a significant fraction of BL Lacs, a new higher limit could classify as BL Lac some "normal" elliptical galaxies. If we assume that all the objects in our sample with K(Ca II)>45% are "normal" elliptical galaxies and that these objects are distributed, in terms of values of Ca II contrast, as the elliptical galaxies studied by Dressler & Shectman (1987) we expect that only 1 - 2 objects among those with a Ca II contrast less than 40% (18 in total) are "normal" galaxies (i.e. $\sim 10\%$). Therefore we call *BL Lac candidates* all the objects without emission lines (EW ≤ 5 Å) and 25%<K(Ca II) $\leq 40\%$. Further observations will be necessary to distinguish the galaxies harbouring a BL Lac nucleus from "normal" galaxies. In section § 8.1 we will present a study of the X-ray luminosities of the BL Lac candidates that supports the hypothesis of the presence of a non-thermal nucleus at least in a fraction of these objects.

Finally, Marchã et al. (1996) proposed a revision also of the limit of 5 Å usually imposed on the equivalent width of the emission lines present in the optical spectrum. Basically, they point out that the observed equivalent width of an emission line is relative to the total continuum that is composed by the thermal emission from the host galaxy plus the non-thermal contribution from the active nucleus. Since the non-thermal nucleus is strongly dependent on the viewing angle, they proposed to refer the intensity of the emission lines to the galaxy starlight. This means that, given a defining limit on the equivalent width of the emission lines (relative to the starlight), the observed equivalent width (i.e. relative to the total emission) depends on the Ca II contrast strength (see Figure 6 of Marchã et al. 1996). We note that a criterium based on the strength of any emission lines relative to the brightness of the host galaxy may introduce in the sample a bias since the same BL Lac nucleus could be differently classified on the basis of the luminosity of the elliptical galaxy that harbours it.

In any case, at present, we have found only one object that fulfills the defining criteria proposed by Marchã et al. (1996) (K(Ca II) \sim 30 % and an emission line - [OII] λ 3727 - with EW \sim 30 Å). The spectrum of this source resembles that of a spiral galaxy Sb or Sc like NGC 4750 or NGC 6643 (see Kennicutt 1992). Thus, we define this object as a "possible" BL Lac but we do not consider it in the analysis of BL Lac candidates presented here.

In summary, we classify an object without strong optical emission lines (EW \leq 5Å) as "firm" BL Lac, if the Ca II contrast is absent or below 25%; as BL Lac candidate, if the Ca II contrast is between 25% and 40%; as elliptical galaxy (usually a radio galaxy, given the high luminosity in the radio band, as described below) if the Ca II contrast is above 40%.

We note that the definition of an object "without emission lines" could be dependent on the observing set-up since the capability of detecting an emission line depends, among other thing, on the actual wavelength coverage. Our spectra cover the range between $\sim 4000\text{Å}$ and $\sim 8000\text{Å}$, extended, in some cases, blue-ward to 3500Å and/or red-ward to 9000Å. An object without emission lines in this range is, in general, a real featureless object. Nevertheless, some objects may show, in a low signal-to-noise spectrum, only a strong H_{α} (see e.g. MS0007.1–0231 in Stocke et

al., 1991). If the redshift of the source is such that the H_{α} emission line falls outside the observed wavelength range, the object could be erroneously classified as "no emission line object". A fraction ($\sim 20\%$) of the objects in the REX survey without emission lines have not been observed in the spectral region where the possible H_{α} is expected. The re-observation of these objects with an adequate wavelength coverage is planned. A similar follow-up will be necessary also for the objects classified from literature (NED).

7. The composition and the general properties of the REX sample

The spectroscopical observations carried out so far have lead to the identification of 125 REX. Another 268 REX have been identified from the literature (NED). Among the 393 REX identified we have found: 202 Emission Line AGNs (67 new), 136 galaxies⁹ (32 new) and 55 BL Lacs or BL Lac candidates (26 new). However, we stress here that the sub-sample of identified REX is not expected to reflect the global composition of the REX sample since it is not a well-defined, representative subset.

At present, the percentage of BL Lac objects in the REX survey is about 14%, and it should be considered only as indicative of the efficiency of the REX survey in finding BL Lacs. Altogether, this number is high if compared with the radio or the X-ray selections. By extrapolating this number, we predict a total of $\gtrsim 200$ BL Lacs that is in fair agreement with the number predicted with our simulations (§ 5.3).

In figure 11 we have reported the radio-optical (α_{RO}) versus the X-ray-optical (α_{OX}) spectral indices of the 393 REX identified so far. Emission line AGNs have been represented as open circles, "firm" BL Lacs as filled circles, BL Lac candidates as filled triangles and galaxies as stars. The values of α_{OX} and α_{RO} have been computed as in Stocke et al. (1991), using the monochromatic fluxes at 5 GHz, 2500Å and 2 keV.

As expected, the majority (84%) of AGNs are radio loud ($\alpha_{RO} \ge 0.35$) but we find also a fraction (16%) of radio quiet AGNs, selected thanks to the low radio flux limit. The percentage of radio quiet AGNs is high in comparison with our simulations (§ 5.3) but we recall that the sample of identified REX is not representative of the whole population and, in particular, it is strongly biased toward the bright magnitudes where the percentage of radio quiet AGNs is expected to be significantly higher. Galaxies are more widely distributed in the α_{RO}/α_{OX} plane; on the other hand, in the case of galaxies in a cluster, a substantial fraction of the X-ray flux probably comes from the intra-cluster gas.

⁹ With the term "galaxy", we intend all the objects defined as such in literature as well as all the elliptical galaxies that follow the criteria presented in § 6. Consequently, this is a quite heterogeneous class, including both "normal" galaxies (spiral or elliptical) and radio galaxies without emission lines in the optical spectrum. To obtain a more precise and homogeneous classification of these objects follow up observations are required.

Figure 11 shows that BL Lac objects occupy a unique area in the α_{RO}/α_{OX} plane, compared to the other classes of sources, as firstly noted by Stocke et al. (1991). Thus, a further selection in terms of α_{RO} , α_{OX} could increase the efficiency of the search for BL Lac objects up to 25-30%. On the other hand, a sample obtained in this way may be biased toward selecting the most "extreme" subset of the whole population.

8. The REX sample of BL Lacs: preliminary results

Although the principal aim of this paper is to present the scientific goals and the selection criteria of the REX survey, two preliminary results can be drawn from the analysis of the current sample of BL Lacs. Since this sample is not complete and representative, given the low rate of identifications, the conclusions must be considered as general indications of the potentiality of this survey.

8.1. The connection between BL Lacs and Radio Galaxies

In the context of the Beaming Model, BL Lac objects and FR I radio galaxies are thought to be the same class of sources seen at different viewing angles (e.g. Urry & Padovani 1995). If this picture is correct, we expect to find some transition objects with intermediate properties between BL Lacs and FR I radio galaxies. Up to now, this intermediate population of objects was missed, probably due to the limiting fluxes of the current X-ray/radio surveys and/or to the criteria adopted to classify a BL Lac. For example, in the Deep X-ray and Radio Blazar Survey (DXRBS, Perlman et al. 1998), which is the result of a positional cross-correlation between the WGA catalog and a number of radio catalogs, an additional constraint on the radio spectral index (i.e. $\alpha_R \leq 0.7$, $f \propto \nu^{-\alpha}$) is imposed to further increase the efficiency of the selection. This constraint excludes from the DXRBS sample most of the "normal" radio galaxies. On the other hand, the presence of both radio galaxies and BL Lac objects in the same sample is of fundamental importance to address the problem of the existence of a population of "transition" objects between "normal" radio galaxies and BL Lacs. The existence of such population of sources is predicted by the beaming model and it is matter of discussion in recent literature (e.g. Browne & Marchã 1993).

In the REX survey we do not impose any further conditions other than the presence of the source in a radio and in an X-ray catalog. Moreover, as described above, we have developed a technique of cross-correlation that allows to select double radio sources (like radio galaxies) as well. For these reasons, we expect that the REX sample will contain both FR I and BL Lacs as well as intermediate objects.

In section 6 we have presented the discovery of low-luminosity BL Lacs that show a value of Ca II contrast intermediate between BL Lacs and elliptical galaxies. To asses if these sources

represent the connection between beamed objects (i.e. BL Lacs) and non-beamed objects (i.e. FR I) we have studied the properties in the X-ray and in the radio band of all the objects for which we detect the Ca II contrast in the optical spectrum (i.e. elliptical galaxies, BL Lac candidates and a fraction of BL Lacs).

The information available for these objects comes from the ROSAT PSPC images and from the NVSS data used to select the REX sample.

Radio properties. The luminosities at 1.4 GHz of the BL Lac candidates and of the elliptical galaxies newly discovered in the REX survey range from 10^{31} to 10^{33} erg s⁻¹ Hz⁻¹, consistent with those of FR I and BL Lacs ($L_R \ge 10^{30}$ erg s⁻¹ Hz⁻¹). Given this range of luminosity, the elliptical galaxies, that do not show any emission line in the optical spectrum, can be classified as radio galaxies, probably FR I. For a fraction of objects we have information on the radio flux at 5 GHz since they are included in the Green Bank catalog (Gregory et al. 1996) or in the PMN catalog (Wright et al. 1994). All the BL Lacs and BL Lac candidates present a slope $\alpha_R \le 0.6$ (fx $\nu^{-\alpha}$) while the radio galaxies cover a wider range of values, from -0.2 to 1.2. The overall distribution of the slopes does not reveal any bimodality.

Radio galaxies and BL Lacs are expected to be different in terms of radio morphology. Typically, a radio galaxy with a radio luminosity between 10^{31} and 10^{33} erg s⁻¹ Hz⁻¹ and a redshift between 0.1 and 0.5 (like the objects discussed here) shows extended radio structures of 100-500 kpc (Singal 1993) while BL Lacs show more compact radio morphologies (Perlman & Stocke 1993; Kollgaard, Gabuzda & Feigelson 1996). These differences cannot be well established with the NVSS data that are characterized by a large beam (FWHM=45") that correspond to a linear size of 100-300 kpc for redshift of 0.1 - 0.5. Specific observations with a better resolution are needed to study the differences between radio galaxies, BL Lacs and BL Lac candidates from the viewpoint of the radio morphology. For the sources falling in the area of sky covered by the FIRST survey we will be able to study the radio morphology with a resolution a factor 10 better than that achieved by the NVSS.

X-ray properties

The X-ray luminosities in the 0.5–2.0 keV band of the radio galaxies and BL Lac candidates are above 3×10^{42} erg s⁻¹. The objects with K(Ca II) \geq 40% (radio galaxies) show X-ray luminosities up to 10^{44} erg s⁻¹ while some of the objects with K(Ca II) \leq 40% (BL Lacs and BL Lac candidates) reach luminosities of 5×10^{44} - 10^{45} erg s⁻¹ consistent (but at the low luminosity end) with the range of luminosities shared by BL Lac objects ($10^{44} < L_X < 10^{47}$ erg s⁻¹). We recall that a typical FR I galaxy (without emission lines in the optical spectrum) hardly reaches X-ray luminosities of 10^{44} erg s⁻¹ (Fabbiano et al. 1984). There are only few cases of objects (Silverman, Harris & Junor 1998; Tananbaum et al. 1997; Caccianiga & Maccacaro 1997) showing high X-ray luminosities ($\geq 3\times10^{43}$ erg s⁻¹) and an optical spectrum without any signature of the presence of an active nucleus (i.e. strong emission lines and/or a reduced value of the Ca II contrast). There are strong evidences that these objects must be considered as BL Lacs whose

optical emission is overwhelmed by the light of the host galaxy.

We note that some of the objects discussed here probably reside in clusters of galaxies and, thus, the X-ray emission could be produced, in part or completely, by the intracluster gas. We have distinguished some of these cases on the basis of CCD observations of the optical field and/or on the basis of spectroscopic observations of other galaxies in the same field.

In Figure 12 we have reported the values of Ca II contrast versus the monochromatic luminosities at 1 keV for the REXs for which we have no evidence of the presence of an overdensity of objects in the optical field (panel a) and for the REX in clusters (panel b). Figure 12a shows that the two quantities are anti-correlated (at >95% confidence level), while clusters of galaxies (Figure 12b) do not show any correlation. The correlation found for the isolated objects suggests a common origin of the high X-ray luminosity and the low value of the Ca II contrast, probably related to the presence of a non-thermal nucleus in the host galaxy: the stronger is the non-thermal emission, the lower is the Ca II contrast and the higher is the X-ray luminosity. In the case of clusters of galaxies, the strong X-ray luminosities are mainly related to the intracluster gas and not to the activity of the nucleus and thus the values of Ca II contrast and the X-ray luminosities are not expected to be correlated.

Figure 12 shows a continuity between the X-ray/optical properties of the radio galaxies and the BL Lac candidates discovered in the REX survey. This continuity suggests that the BL Lac candidates represents the connection between BL Lacs and their parent population. In the context of the beaming model, these sources could be less beamed than the "usual" BL Lac objects i.e. they are seen at viewing angles intermediate between FR I ($\sim 90^{\circ}$) and BL Lacs ($\sim 0^{\circ} - 30^{\circ}$).

We note that, given the modest angular resolution achieved by the PSPC instrument, in particular at large offaxis angles (>20'), we are not able to exclude the presence of a diffuse contribution to the X-ray luminosity also for the objects for which we do not detect the presence of an overdensity of galaxies in the optical field. More accurate and spatially resolved X-ray observations (e.g. with ROSAT HRI or AXAF) are needed in order to unambiguously assess the presence of a point-like source among the BL Lac candidates.

8.2. XBL versus RBL

Up to now, radio and X-ray surveys have selected different types of BL Lacs, called RBL and XBL, respectively. Typically, XBLs are less variable and less polarized than RBLs. The overall spectral distribution of the two classes is strongly bimodal and their cosmological evolution differs significantly (Morris et al. 1991; Stickel et al. 1991; Wolter et al. 1994; Bade et al. 1998). Moreover, XBLs frequently show absorption features in their optical spectrum similar to those of "normal" elliptical galaxies. This is an indication that the contribution of the non-thermal emission, coming from the nucleus (or the jet), is not strong enough to cancel completely the stellar emission from the host galaxy. The existence of two distinct populations of BL Lacs was

tentatively attributed to a difference in the width of the emission cones of the radio and X-ray radiation (Ghisellini & Maraschi 1989; Celotti et al. 1993): in this framework, the X-ray radiation is less beamed than the radio one and, consequently, XBLs are seen at angles larger than the RBLs. Nevertheless, Sambruna et al. (1996) have shown that the typical radio-to-X-ray spectrum of an XBL cannot be obtained from the spectrum of an RBL simply by changing the viewing angle alone and they suggested that other physical parameters, like the intensity of the magnetic fields, must be considered. Moreover, XBLs and RBLs show significant differences in the slope of their X-ray spectra (Comastri, Molendi & Ghisellini 1995; Urry et al. 1996; Padovani & Giommi 1996; Lamer, Brunner & Staubert 1996) that are difficult to explain in terms of a different viewing angle. Giommi & Padovani (1994) have suggested the existence of a unique class of BL Lacs, characterized by a wide range of different overall spectral properties. The X-ray and radio surveys have sampled the extreme ends of this distribution thus creating an apparent dichotomy: the class of High energy peaked BL Lacs (HBL~XBL) and the class of Low energy peaked BL Lacs (LBL~RBL). In this framework, the intermediate objects between HBL and LBL were missed in previous X-ray and radio surveys. Recently, Fossati et al. (1997) have elaborated further the idea proposed by Giommi & Padovani (1994), suggesting that the physical parameter which governs the shape of the spectral distribution is the bolometric luminosity.

The most compelling and straightforward way to test these competing hypothesis is to select a new sizable sample of BL Lacs containing both HBL and LBL, in order to compare directly their properties. At present, the only existing statistically complete samples of BL Lacs contain only few tens of objects each. Since the REX survey reaches radio fluxes 200 times fainter than the limiting flux of the 1 Jy sample and X-ray fluxes about 10 times below the EMSS limits, we expect to find both kinds of BL Lacs as well as objects with intermediate properties. We have shown the results of numerical simulations to evaluate the capability of the REX survey to select LBLs and HBLs and, as described above, we have found that both kinds of objects are expected to be sampled.

In Figure 13 we show the α_{RX} distribution for the 55 BL Lacs (or BL Lac candidates) discovered in the REX survey. The shaded histogram represents only the "firm" BL Lacs. This figure does not reveal any bimodality. Nearly all the BL Lacs of this sample (47/55) fall below the limit on α_{RX} frequently used to discriminate between HBL and LBL ($\alpha_{RX}=0.8$, e.g. Padovani & Giommi 1996). Apparently, the number of HBL largely exceeds that of LBLs, as suggested by the "viewing angles hypothesis" or the "bolometric" scenario proposed by Fossati et al. (1997). Moreover, Figure 13 shows that several BL Lacs (13) are intermediate (0.70 $\leq \alpha_{RX} \leq 0.80$) between the BL Lacs of the EMSS ($\alpha_{RX} \leq 0.70$) and that of the 1 Jy sample ($\alpha_{RX} \geq 0.8$). This result seems to rule out the models proposed by Ghisellini & Maraschi (1989) or by Celotti et al. (1993) that predict a sharp separation between LBLs and HBLs, and to support those models that predict a smooth passage between LBLs and HBLs, like those proposed by Giommi & Padovani (1994) or by Fossati et al. (1997). However, the incidence of both the radio and the X-ray limits in the selection must be considered before drawing any firm conclusion about the relative number

of HBL and LBL. The sky coverage of the REX survey, in fact, is the combination of the limiting fluxes in the X-ray and in the radio band. Other projects, similar to the REX survey, find samples of BL Lacs very different in terms of HBL/LBL ratio: for example, the DXRBS (Perlman et al. 1998) finds a low number of HBL object (16%) in comparison with the intermediate and the LBL objects (84%). Conversely, the RASS-Green Bank sample (RGB, Laurent-Muehleisen et al. 1998) contains mostly HBL (\sim 60%) and intermediate (\sim 23%) objects while only the \sim 17% is composed by LBLs. Finally, about half of the RC sample (Kock et al. 1996) are HBL and about half are intermediate objects.

These results clearly show the importance of the radio/X-ray limits in the sampling of the BL Lac population: the DXRBS is characterized by a high ratio between the radio and the X-ray limiting fluxes ($\alpha_{RX} \sim 0.8$ –0.9) and, thus, it favours the selection of the LBL, while the RGB and the REX surveys are more shifted toward lower ratio between radio/X-ray limiting fluxes ($\alpha_{RX} \sim 0.6$ –0.7) and, for this reason, they are able to sample the HBL population.

A way to take into account these selection effects is to compare the spatial densities of the two populations of BL Lacs, i.e. the number of objects divided by the volume of universe sampled (which must be computed by taking into account the limiting fluxes in the two selection bands). Alternatively, it is possible to use the competing theoretical models proposed and the radio and X-ray sky-coverage of the REX sample to predict the number of BL Lacs expected in the survey. Then, through a comparison between the predicted and the observed number of HBL/LBL it will be possible to draw some interesting conclusions about the origin of the BL Lac dichotomy. At this stage, however, given the low identification rate of the sample, we cannot perform any detailed statistical analysis on the ratio HBL/LBL.

9. Summary and conclusions

We have presented and discussed in detail the scientific goals and the selection criteria of the REX Survey, a project optimized for the selection of new, large samples of BL Lacs and Radio Loud AGNs over a large area of sky (2183 deg²). Since the existing X-ray catalogs obtained from the pointed PSPC observations are not suitable for statistical studies we have produced our own X-ray catalogue from the analysis of a well defined subset of all the public PSPC images using a source detection and characterization algorithm based on wavelet transforms (Damiani et al. 1997a, 1997b). An elaborate positional cross-correlation between this newly compiled catalog of X-ray sources and the NVSS (Condon et al. 1998) radio catalog has led to the definition of about 1450 "single component" REX, 90 REX that show a radio double or triple morphology and about 180 T-REX that still need to be correctly classified. Upon classification of the remaining T-REX, the final number of REXs will be close to 1600 (including the objects with a complex radio morphology). The positional accuracy of the VLA allows us, in the very large majority of cases, to unambiguously identify the optical counterpart of the radio emitting X-ray source, making feasible a program aimed at the complete identification of the whole sample.

The REX sample contains a very high fraction of RL AGNs and BL Lac objects as indicated by preliminary results of the optical identification program.

The high number of BL Lacs expected in the survey (≥ 200) will increase significantly our knowledge of their nature and statistical properties currently based on samples of a few tens of objects. Moreover, the possibility of comparing directly in the same sample the properties of "XBL" and "RBL" will be instrumental in testing the existing theoretical emission models.

Finally, unlike other similar projects (e.g. the DXRBS), in the REX survey we do not impose any constraint on the slope of the radio spectrum. In this way we will be able to compare directly radio galaxies and BL Lacs in the same sample and to test the transition between a "normal" radio galaxy and a BL Lac object. The importance of this characteristic is confirmed by the preliminary results presented in this paper. We have analyzed a sample of newly discovered BL Lac and elliptical galaxies for which we have an homogeneous set of optical spectra. Given the high luminosities at 1.4 GHz ($\geq 10^{31} \text{ erg s}^{-1}$), the elliptical galaxies, that do not show any emission line in their optical spectrum, can be considered as radio galaxies, probably FR I. In the optical band we have found that the distinction between BL Lacs and elliptical galaxies is quite blurred. In the X-ray band, both radio galaxies and BL Lacs show a significant anti-correlation between the X-ray luminosity and the value of the Ca II contrast (which is an indicator of the fraction between the stellar and the nuclear emission in the optical band). The radio galaxies show higher values of Ca II contrast ($\sim 50\%$) and lower X-ray luminosities ($< 5 \times 10^{43} \text{ erg s}^{-1}$) while BL Lacs show lower values of Ca II contrast ($\leq 40\%$) and higher X-ray luminosities ($> 5 \times 10^{43} \text{ erg s}^{-1}$). This behavior could be interpreted as due to an increasing importance of the nuclear non-thermal components in these sources. This can be connected either to the intrinsic power of the non-thermal nucleus or to the effect of orientation in the framework of the beaming model.

We thank F. Damiani and S. Sciortino for providing us with their source-detection algorithm and for useful discussions and C. Ruscica for his contribution in the early stage of this work. We also thank the referee Simon Morris for constructive criticisms and suggestions that significantly improved the quality of the paper. J.J.Condon was always very responsive in helping us understand all the details of the NVSS. This research has made use of the NASA/IPAC extragalactic database (NED), which is operated by the JET Propulsion Laboratory, Caltech under contract with the National Aeronautics and Space Administration. We would like to thank the staff of the Laboratory for High Energy Astrophysics (LHEA) at NASA/GSFC for their efforts to maintain the ROSAT archive. This work has received partial financial support from the Italian Space Agency (ASI), from NASA (NASA grant GO-5402.01-93A, GO-05987.02.94A, NAG5-2594, NAG5-2914) and from NSF (NSF grant AST95-00515).

Bade, N., Beckmann, V., Douglas, N. G., Barthel, P. D., Engels, D., Cordis, L., Nass, P., & Voges, W. 1998, MNRAS, in press

Becker, R. H., White, R. L., & Helfand, D. J. 1995, ApJ, 450, 559

Boyle, B. J., Shanks, T., Georgantopulos, I., Stewart, G. C., & Griffiths, R.E. 1994, MNRAS, 271, 639

Brinkmann, W., Yuan, W., & Siebert, J. 1997, A&A, 319, 413

Browne, I. W. A., & Marchã, M. J. M. 1993, MNRAS, 261, 795

Caccianiga, A., & Maccacaro, T. 1997, AJ, 114, 2350

Celotti, A., Maraschi, L., Ghisellini, G., Caccianiga, A., & Maccacaro, T. 1993, ApJ, 416, 118

Comastri, A., Molendi, S., & Ghisellini, G. 1995, MNRAS, 277, 297

Condon, J. J., Cotton, W. D., Greisen, E. W., Yin, Q. F., Perley, R. A., Taylor, G. B., & Broderick, J. J. 1998, AJ, 115, 1693

Damiani, F., Maggio, A., Micela, & G., Sciortino, S. 1997a, ApJ, 483, 350

Damiani, F., Maggio, A., Micela, & G., Sciortino, S. 1997b, ApJ, 483, 370

Della Ceca, R., Zamorani, G., Maccacaro, T., Wolter, A., Griffiths, R., Stocke, J. T. & Setti, G. 1994, ApJ, 430, 533

Dickey, J. M. & Lockman, F. J. 1990, ARA&A, 28, 215

Dressler, A., & Shectman, S. 1987, AJ, 94, 899

Fabbiano, G., Miller, L., Trinchieri, G., Longair, M., & Elvis, M. 1984, ApJ, 277, 115

Fossati, G., Celotti, A., Ghisellini, G., & Maraschi, L. 1997, MNRAS, 289, 136

Ghisellini, G., & Maraschi, L. 1989, ApJ, 340, 181

Giommi, P., & Padovani, P. 1994, MNRAS, 268, L51

Gregg, M. D., Becker, R. H., White, R. L., Helfand, D. J., McMahon, R. G., & Hook, I. M. 1996, AJ, 112, 407

Gregory, P. C., Scott, W. K., Douglas, K., & Condon, J. J. 1996, ApJS, 103, 427

Kennicutt, R. C. 1992, ApJS, 79, 255

Kock, A., Meisenheimer, K., Brinkmann, W., Neumann, M., & Siebert, J. 1996, A&A, 307, 745

Kollgaard, R. I., Gabuzda, D. C., & Feigelson, E. D. 1996, ApJ, 460, 174

Lamer, G., Brunner, H., & Staubert, R. 1996, A&A, 311, 384

Laurent-Muehleisen, S. A., Kollgaard, R. I., Ciardullo, R. Feigelson, E. D., Brinkmann, W., & Siebert, J. 1998, ApJS, in press

Maccacaro, T. et al. 1994, Astrophys. Lett. Comm. 29, 267

Marchã, M. J. M., Browne, I. W. A., Impey, C. D., & Smith, P. S. 1996, MNRAS, 281, 425

Morris, S. M., Stocke, J. T., Gioia, I. M., Schild, E., Wolter, A., Maccacaro, T., & Della Ceca, R. 1991, ApJ, 380, 49

Nass, P., Bade, N., Kollgaard, R.I., Laurent-Muehleisen, S. A., Reimers, D., & Voges, W. 1996, A&A, 309, 419

Owen, F. N., Ledlow, M. J. & Keel, W. C. 1996, AJ, 111, 53

Padovani, P., & Giommi, P. 1995, ApJ, 444, 567

Padovani, P., & Giommi, P. 1996, MNRAS, 279, 526

Page, M. J., et al. 1996, MNRAS, 281, 579

Perlman, E., Padovani, P., Giommi, P., Sambruna, R., Jones, L. R., Tzioumis, A., & Reynolds, J. 1998, AJ, in press

Perlman, E., & Stocke, J. T. 1993, ApJ, 406, 430

Perryman, M. A. C. et al. 1997, A&A, 323, 49

Rosati, P., Della Ceca R., Burg, R., Norman, C. & Giacconi, R. 1995 ApJ, 445, L11

Sambruna, R. M., Maraschi, L., & Urry, C. M. 1996, ApJ, 463, 444

Silverman, J. D., Harris, D. E., & Junor, W. 1998, A&A, 335, 443

Stickel, M., Padovani, P., Urry, C. M., Fried, J. W., & Kühr, H. 1991, ApJ, 374, 431

Stocke, J. T., Morris, S. L., Gioia, I. M., Maccacaro, T., Schild, R. E & Wolter, A. 1990, ApJ, 348, 141

Stocke, J. T., Morris, L. M., Gioia, I. M., Maccacaro, T., Schild, R., Wolter, A., Fleming, T.A., & Henry, J. P. 1991, ApJS, 76, 813

Tananbaum, H., Tucker, W., Prestwich, A., & Remillard, R. 1997, ApJ, 476, 83

Urry, C. M., & Padovani, P. 1995, PASP, 107, 803

Urry, C. M., Sambruna, R. M., Worral, D. M., Kollgaard, R. I., Feigelson, E. D., Perlman, E. S., & Stocke, J. T. 1996, ApJ, 463, 424

Veilleux, S., & Osterbrock, E. 1987, ApJS, 63, 295

Véron-Cetty, M.-P., & Véron, P. 1996, ESO Scientific Report 17

Vikhlinin, A., Forman, W., Jones, C., & Murray, S. 1995, ApJ, 451, 553

Voges, W. 1993, Adv. in Space Research, vol. 13, n. 12, p. 391

Voges, W., et al. 1996, IAU Circular No. 6420

Wilson, A. S., & Colbert, E. J. M. 1995, ApJ, 438, 62

Wolter, A., Caccianiga, A., Della Ceca, R., & Maccacaro, T. 1994, ApJ, 433, 29

Wolter, A., Ruscica, C., & Caccianiga, A. 1998, MNRAS, in press

Wright, A. E., Griffith, M. R., Burke, B. F., & Ekers, R. D. 1994, ApJS, 91, 111

Wurtz, R., Stocke, J. T., Ellingson, E., & Yee, H. K. C. 1997, ApJ, 480, 547

This preprint was prepared with the AAS LATEX macros v4.0.

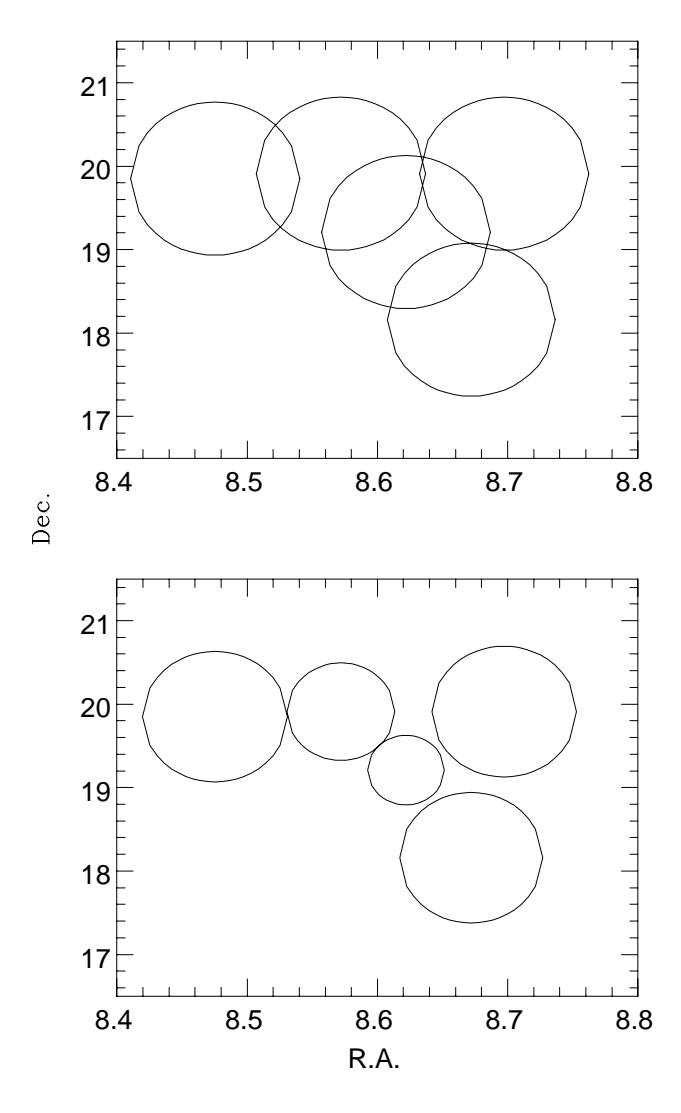


Fig. 1.— (a) An example of overlap of PSPC fields. (b) The same region of sky after the cleaning procedure that produces a set of completely disjointed fields albeit of reduced size. Although this procedure does not maximize the area of sky covered (the region among the fields is not completely covered) it simplifies the source detection procedure that is applied on a set of totally independent fields. We also recall that a maximum radius of 47' is used for the useful area of a PSPC image.

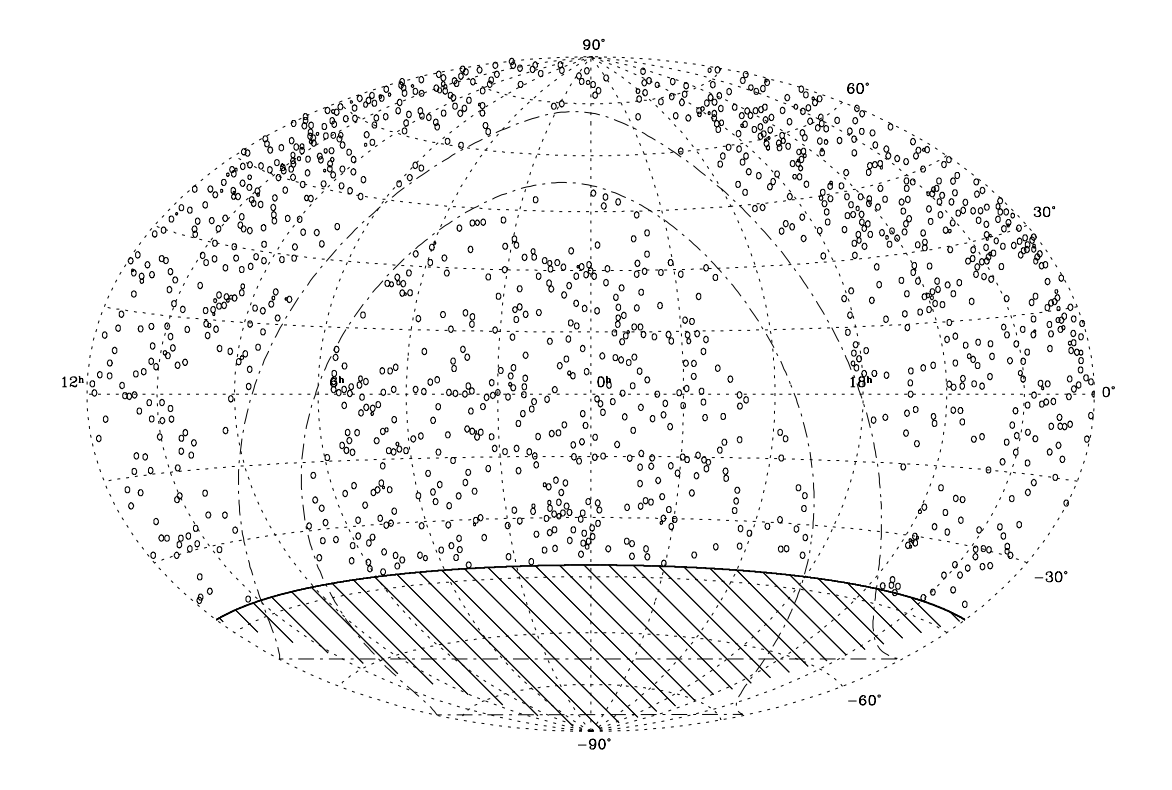


Fig. 2.— Sky distribution of the PSPC fields used for the REX project.

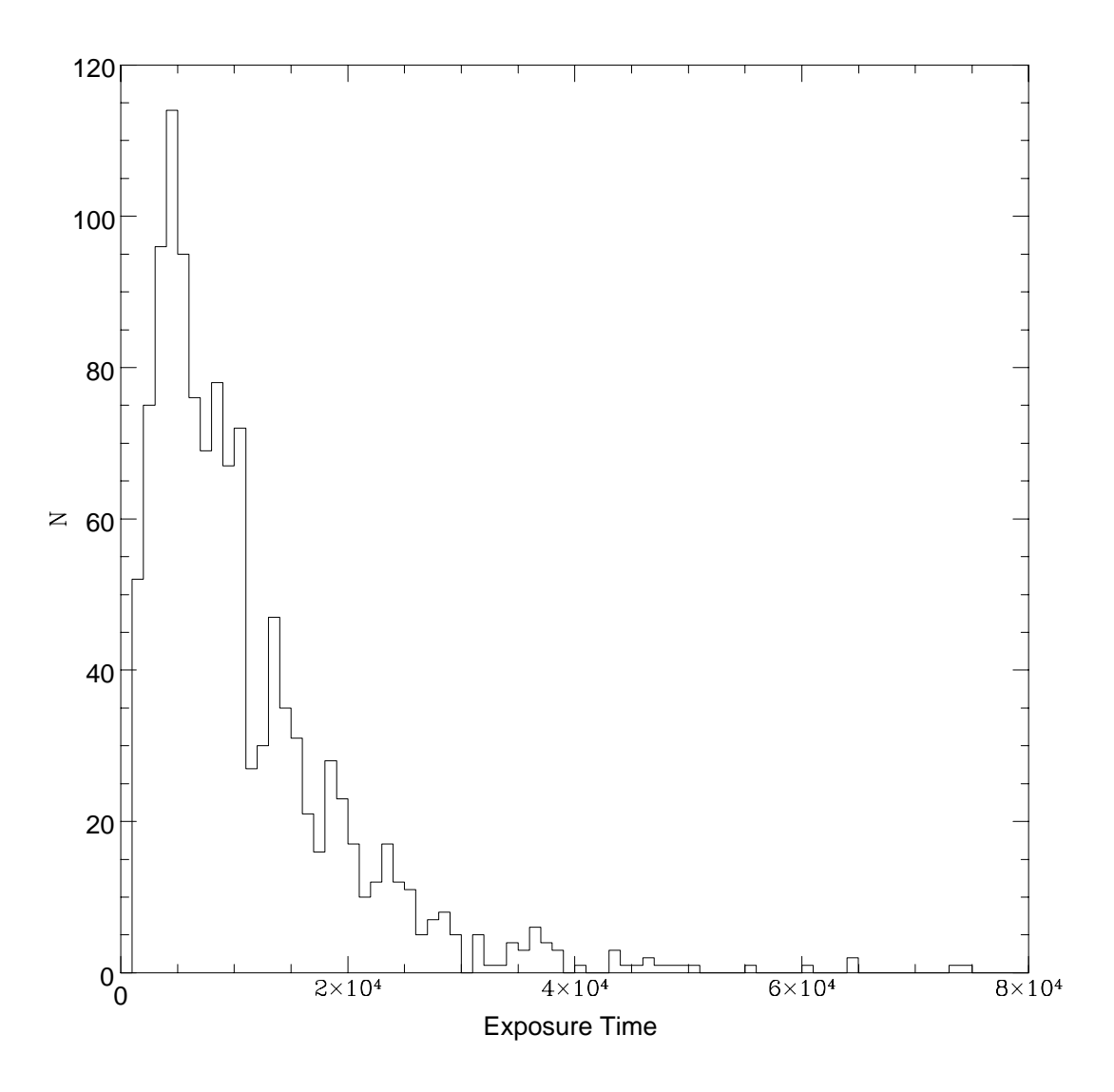


Fig. 3.— The histogram of the exposure times of the used PSPC fields

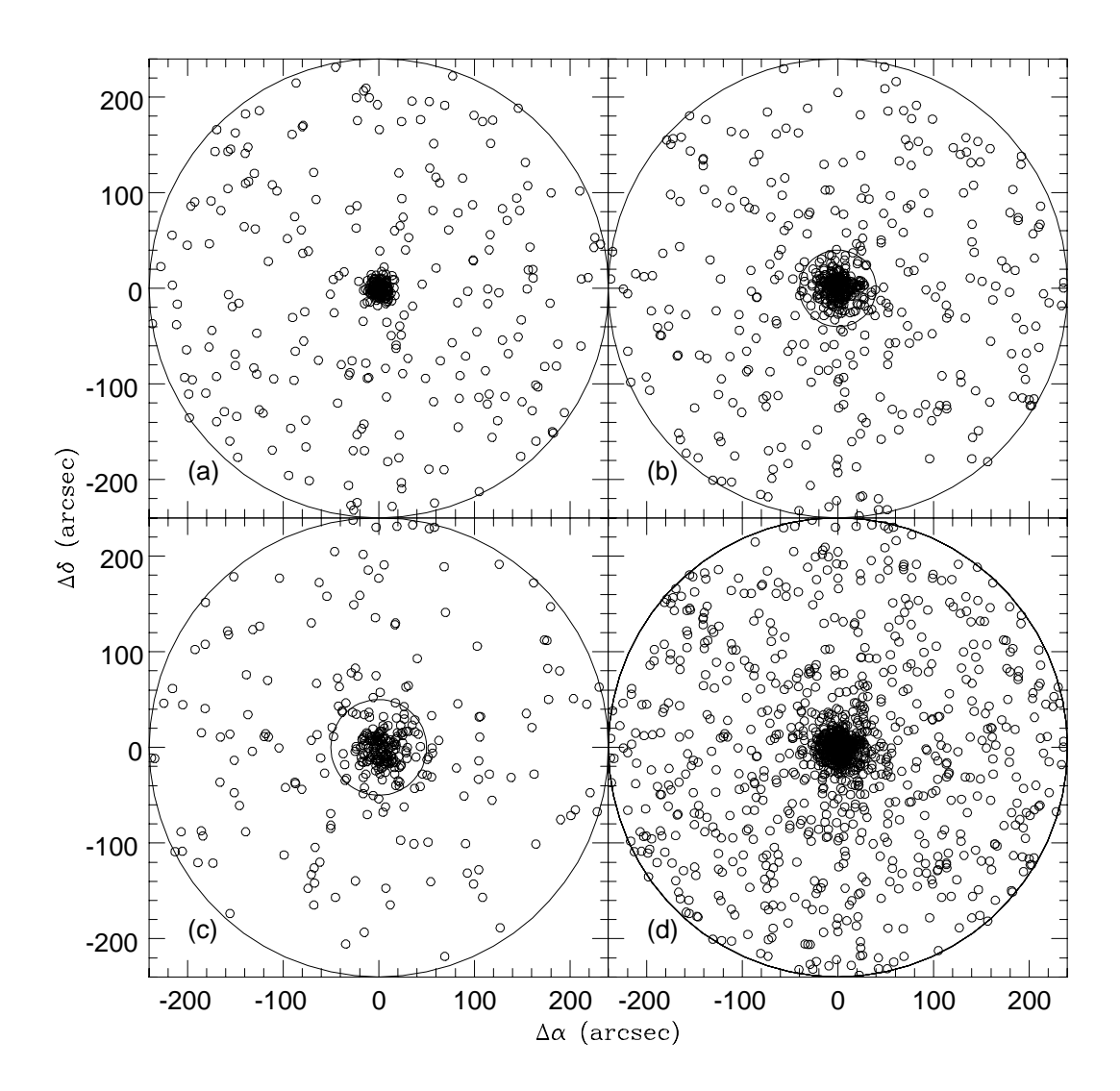


Fig. 4.— The distribution of the offsets between the position of AGNs and stars in the V&V96 and HIC catalogs and the X-ray position from our catalog. The first three panels correspond to three different ranges of the offaxis angle in the ROSAT PSPC field: (a) from 0' to 19'; (b) from 19' to 35'; (c) from 35' to 47'. In (d) are reported all the 1485 correlations. The circles of radius $r_{90}=14''$, 40" and 50" plotted in (a), (b) and (c) represent the 90% X-ray error circles derived from the analysis presented in the text.

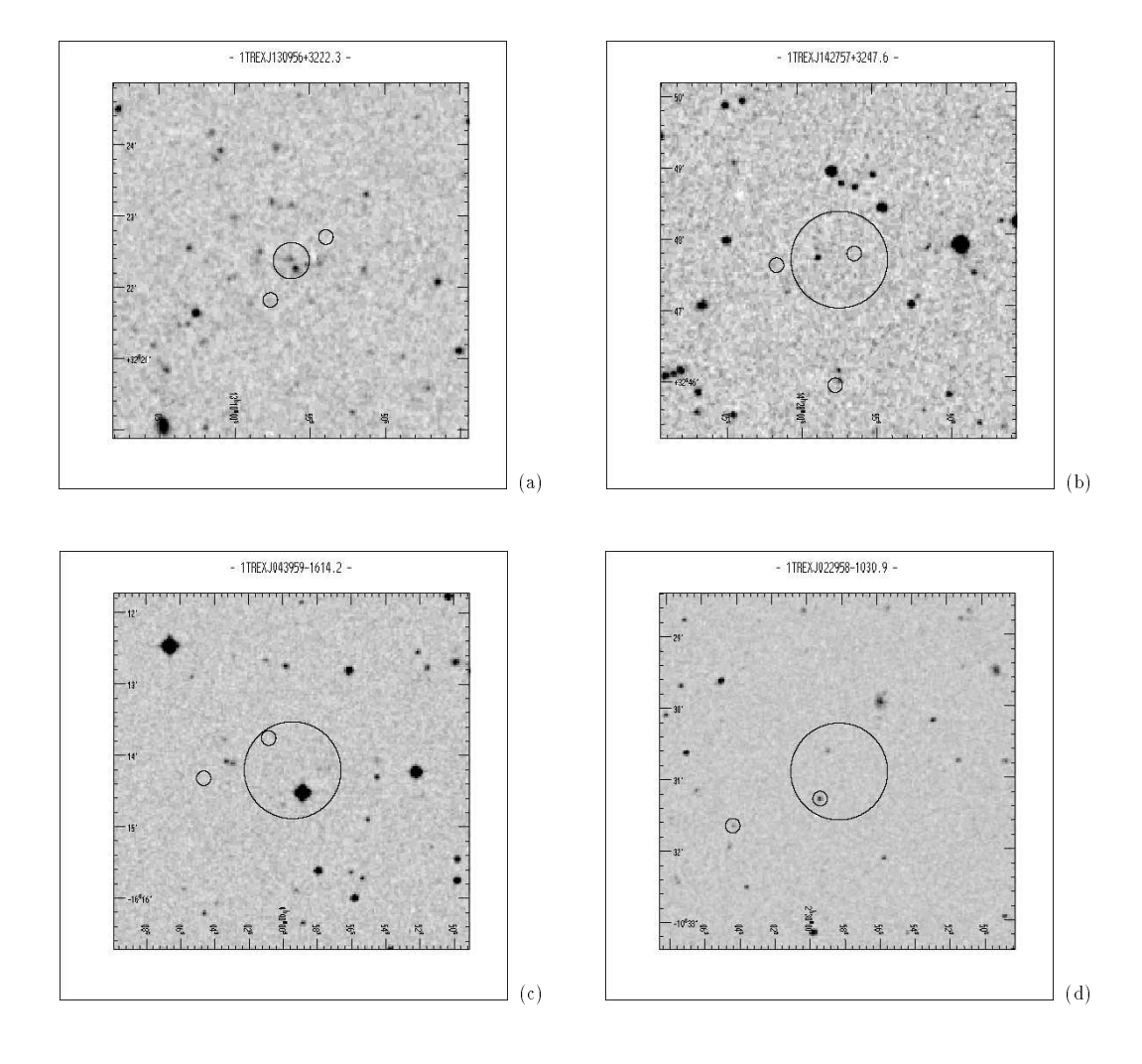


Fig. 5.— (a) An example of REX that would be totally lost in a "blind" cross-correlation between radio (small circles) and X-ray (large circle) positions; (b) An example of an extended radio source which may introduce an erroneous identification of the optical counterpart; (c) An example of an

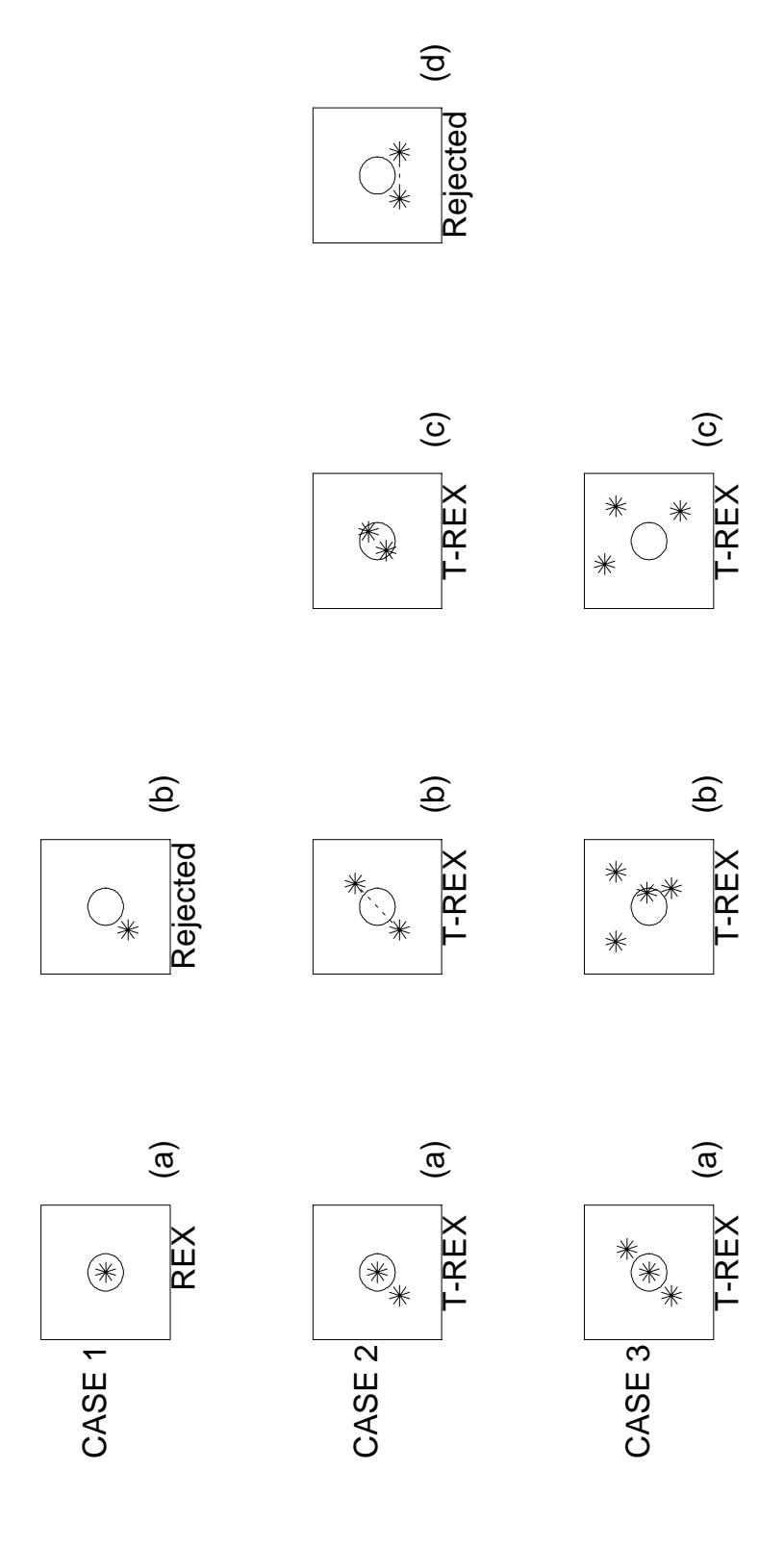


Fig. 6.— Possible configurations resulting from the cross-correlation between radio sources (indicated with stars) and X-ray sources (small circles), using an impact parameter of 2.5′ (box). There are three possible cases: 1 - only one radio source falls closer than 2.5′ to an X-ray source; 2 - two radio sources fall closer than 2.5′ to a X-ray source; 3 - three or more sources fall closer than

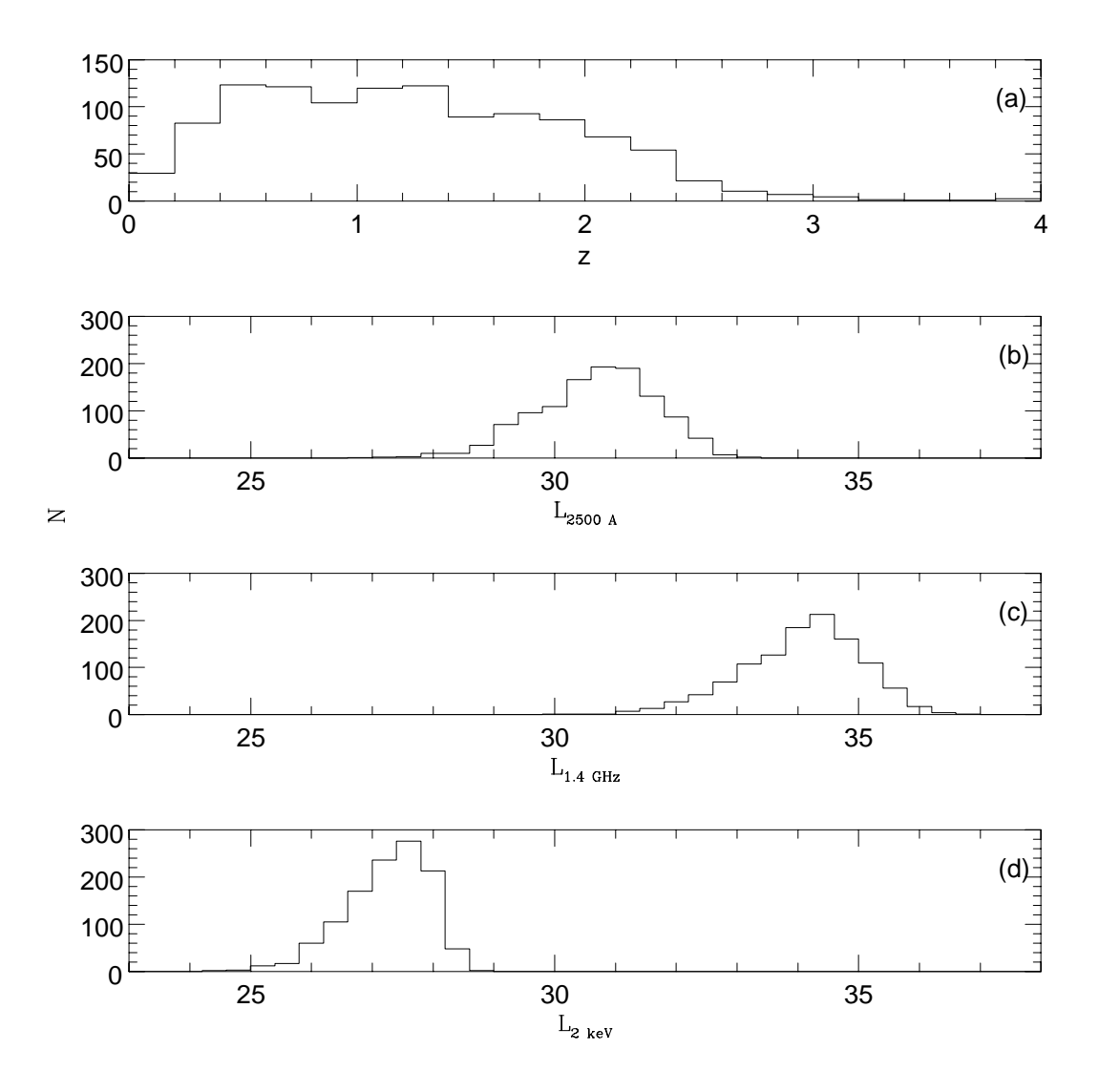


Fig. 7.— The distribution of redshift (a), optical (b), radio (c) and X-ray (d) monochromatic luminosities of the simulated sample of RL AGNs.

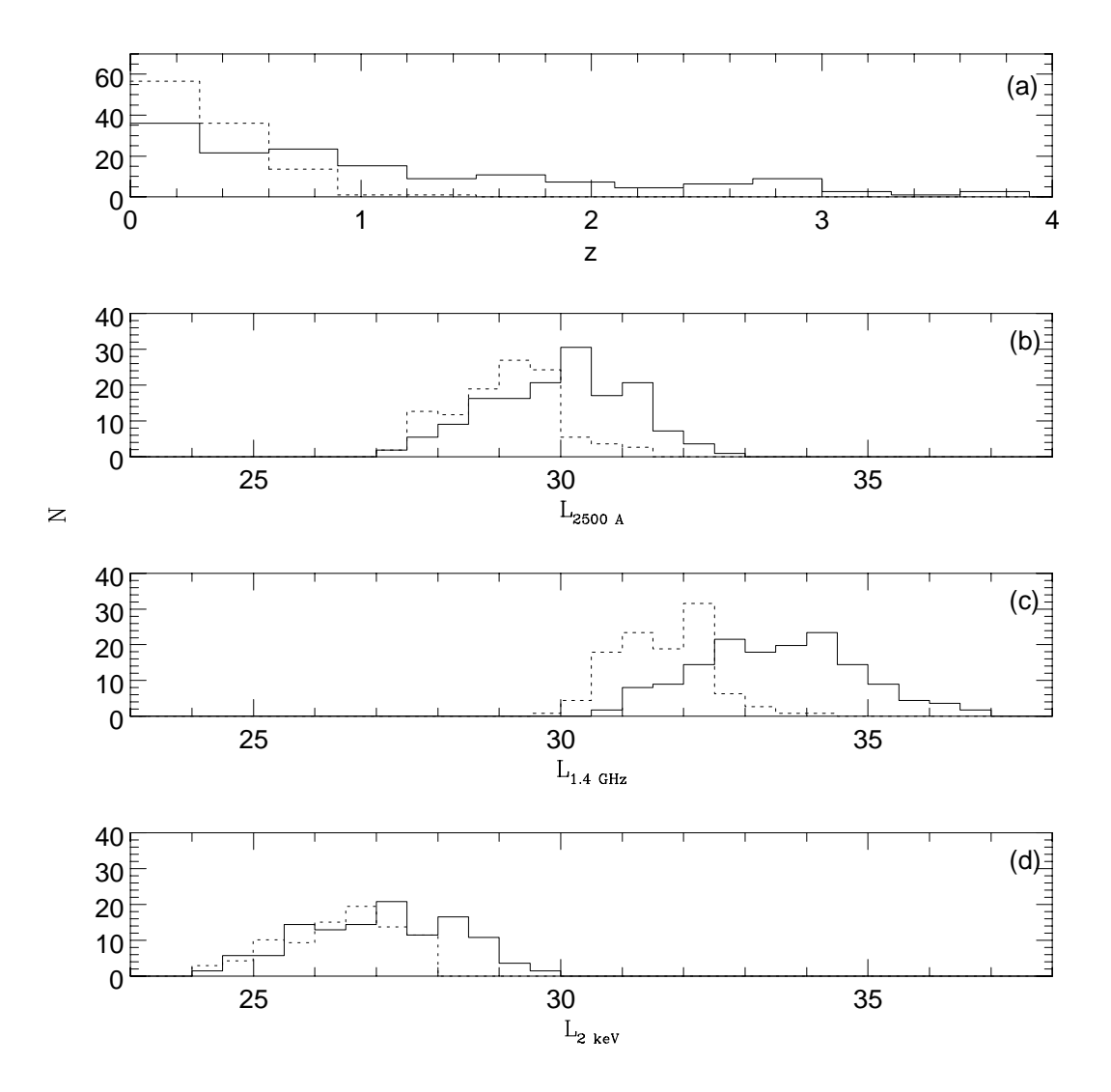


Fig. 8.— The distribution of redshift (a), optical (b), radio (c) and X-ray (d) monochromatic luminosities of the simulated sample of BL Lacs, divided into "RBL-type" (continuous line) and "XBL-type" (dashed lines).

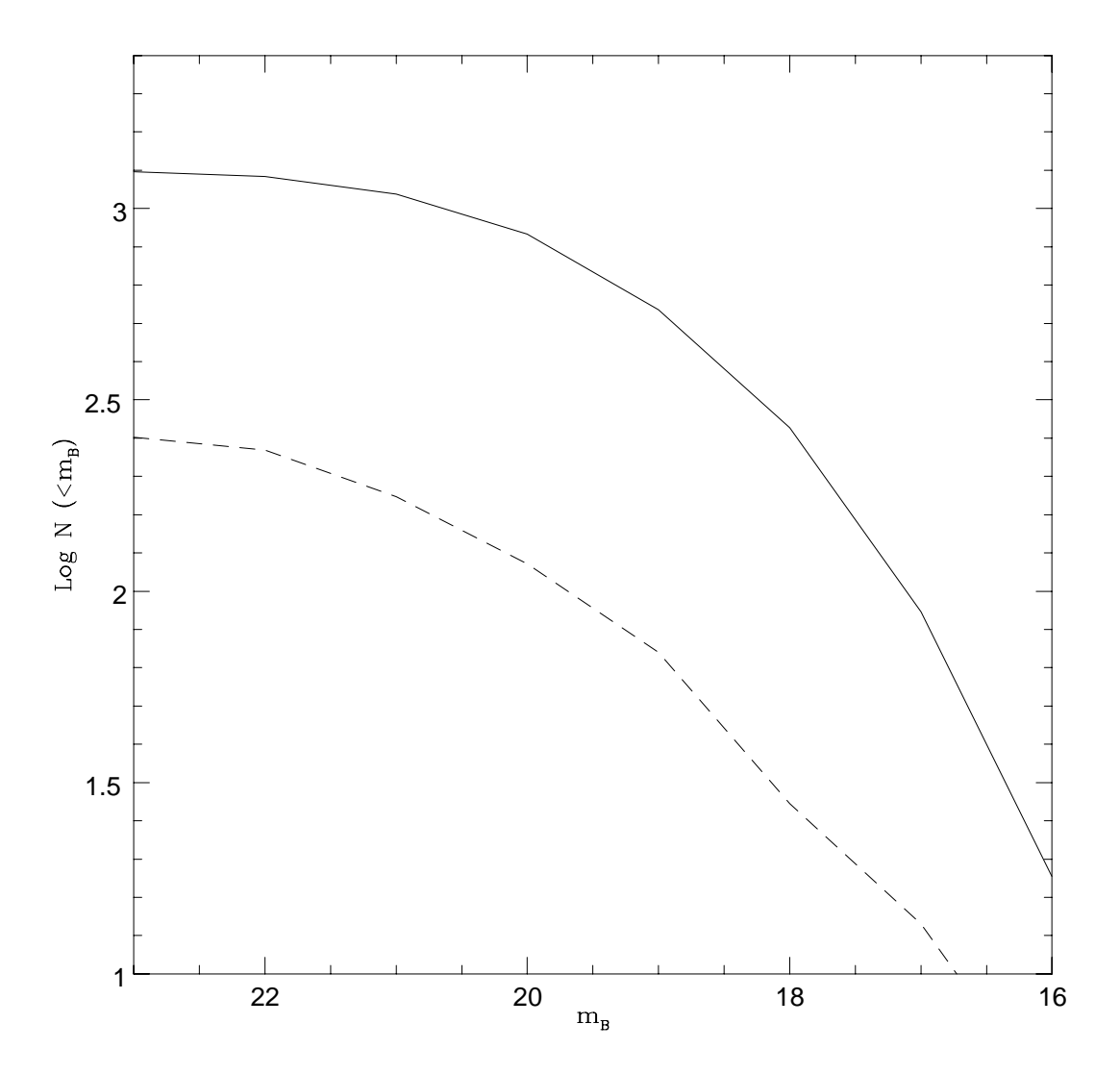


Fig. 9.— The logarithm of the expected number of AGNs, both radio loud and radio quiet (continuous line) and BL Lac objects (dashed line) present in the REX sample, as a function of the B magnitude.

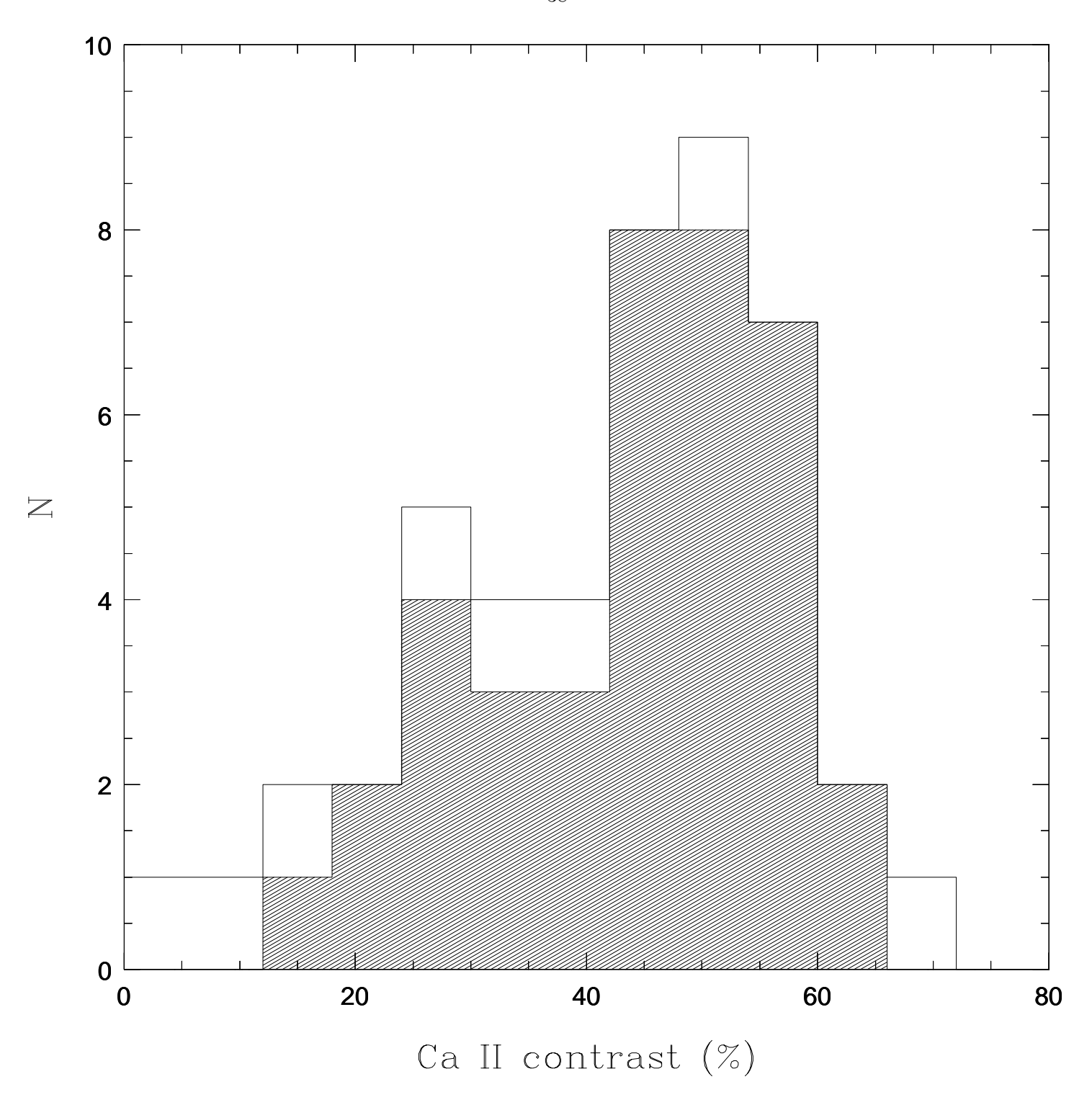


Fig. 10.— The distribution of Ca II contrast of the objects without optical emission lines discovered in the REX survey. The shaded histogram represents only the objects with a firm estimate of redshift.

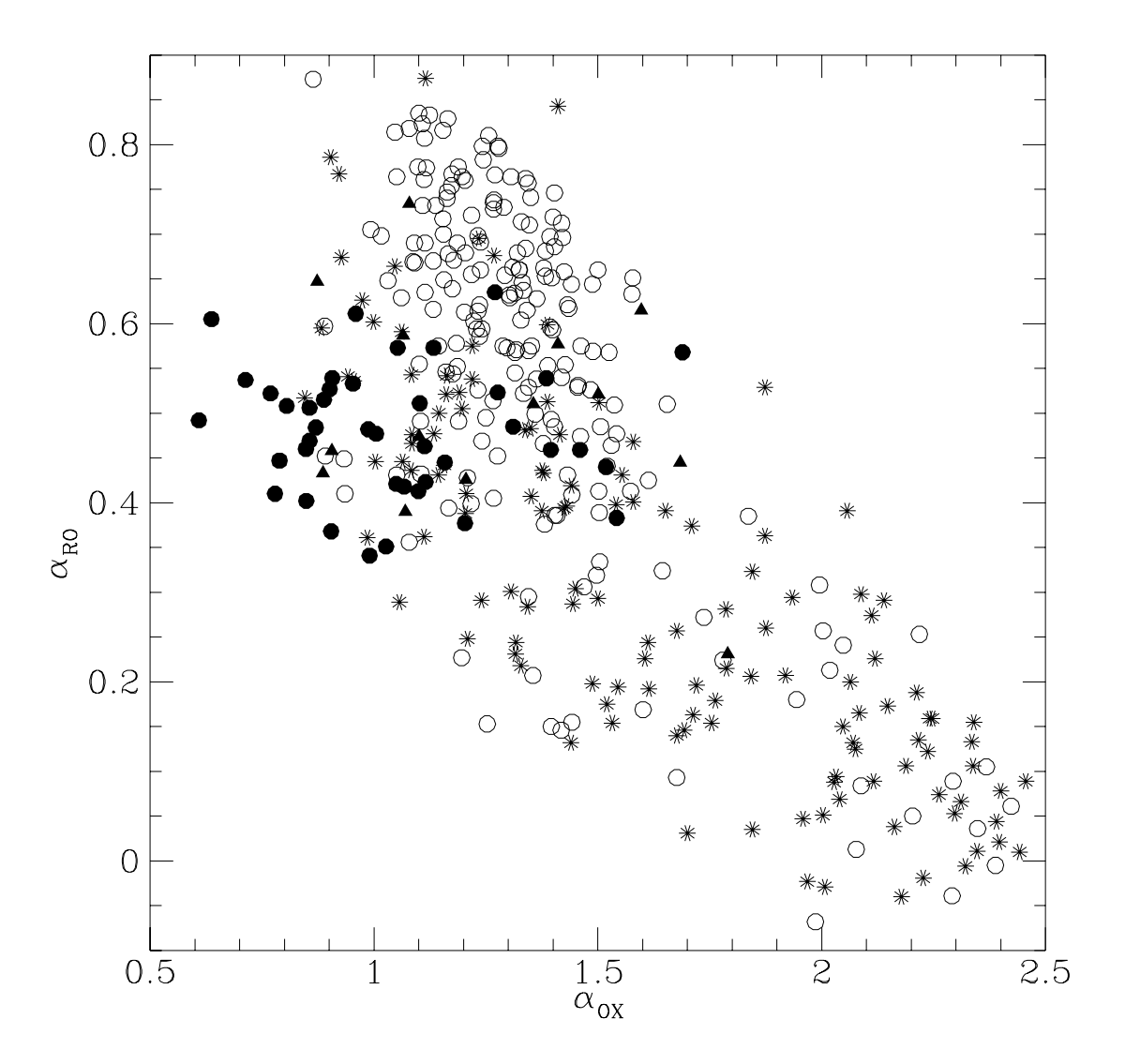


Fig. 11.— The radio-optical (α_{RO}) versus the X-ray-optical (α_{OX}) spectral indices of the 393 REX identified. Emission line AGNs are represented as open circles, "firm" BL Lacs as filled circles, BL Lac candidates as filled triangles and galaxies as stars.

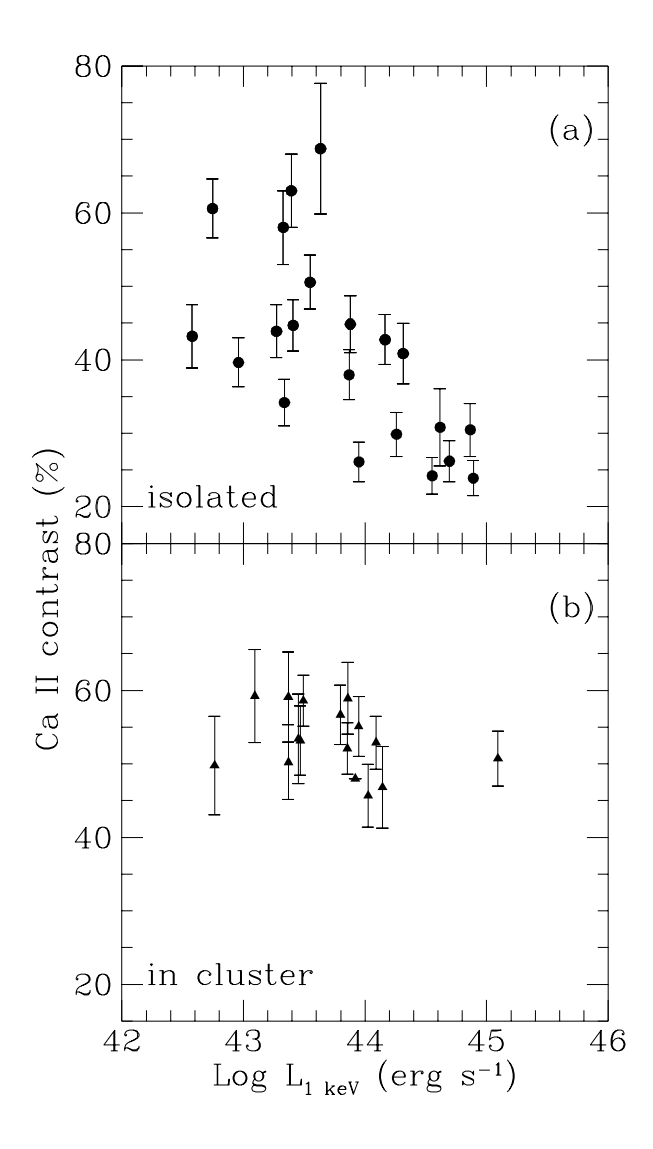


Fig. 12.— The value of Ca II contrast versus the monochromatic X-ray luminosity at 1 keV for the elliptical galaxies and BL Lac candidates newly discovered in the REX survey. We have distinguished, on the basis of the optical images, the objects for which there are no evidences for the presence of a cluster of galaxies (a) from possible clusters (b). Only the objects with a firm estimate of redshift have been considered.

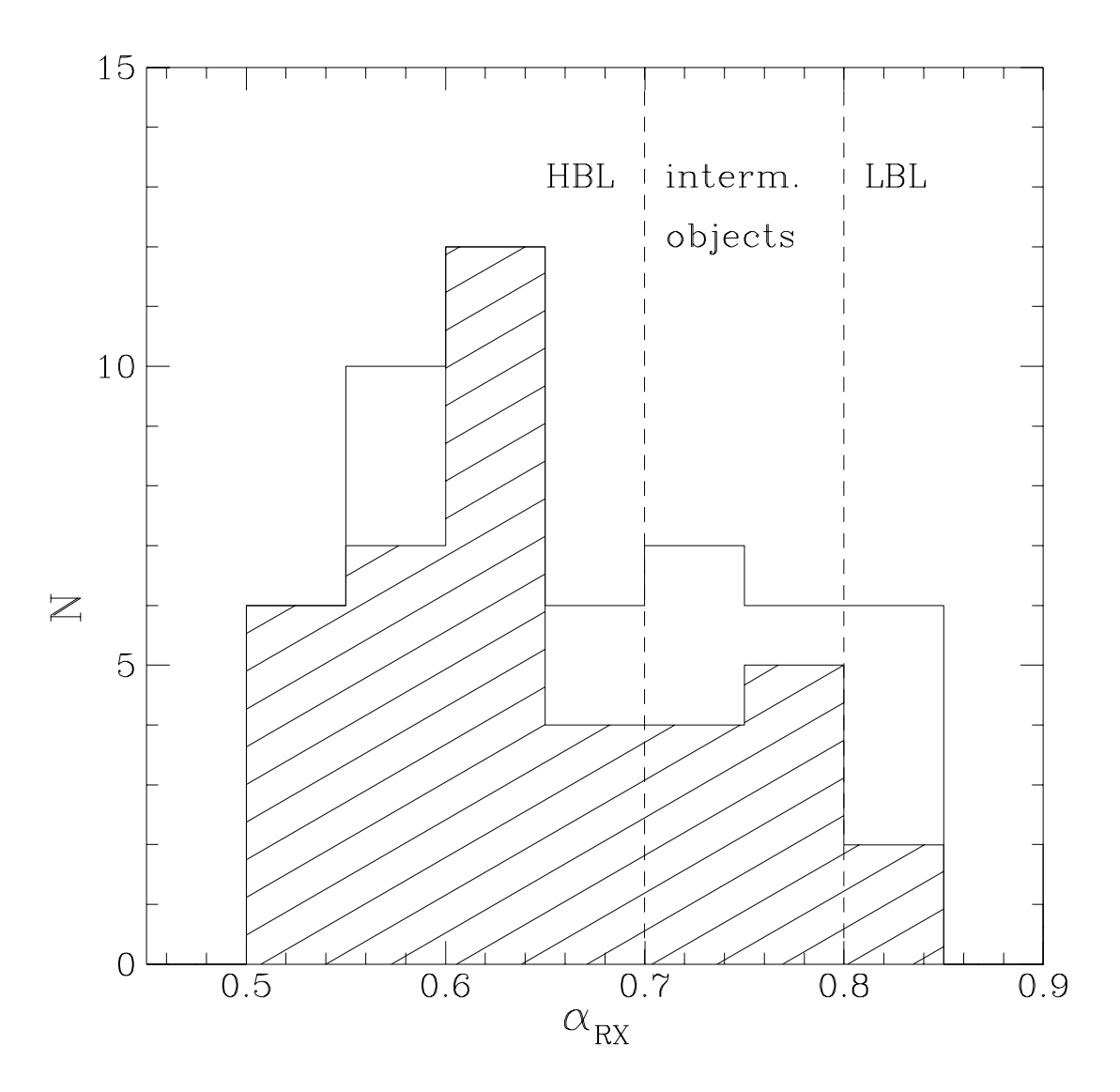


Fig. 13.— The distribution of the α_{RX} of the BL Lacs in the REX sample. The shaded area represents only the "firm" BL Lacs, i.e. the objects with a Ca II contrast below 25% (see text for details).

Table 1. Observing setup

Telescope/Instrument	Grism name (g/mm)	Slita	Dispersion ^b	Observing Period
UNAM 2.1m + BC UNAM 2.1m + BC UH 88" + WFGS UH 88" + WFGS UNAM 2.1m + BC ESO 2.2m + EFOSC2 ESO 3.6m + EFOSC1 UH 88" + WFGS	(300) (300) blue (400) green (420) (300) n.1 (100), n.6 (300) B300 (300), R300 (300) blue (400)	1.6 1.5 2.3 1.6 1.5 1.5	3.9 3.9 4.2 3.7 3.9 13.2, 4.1 6.3, 7.5 4.2	1995 Apr 25–27 1995 Sep 22–24 1996 Jan 14–15 1996 Aug 7–11 1996 Dec 6–10 1996 Dec 11–12 1996 Dec 9–10 1997 Mar 3–5
UH 88"+ WFGS	blue (400)	1.5	4.2	1998 Feb 26 - Mar 1

^ain arcseconds

 $^{^{\}rm b}$ in Å/pixel